

# Resonances and Continuum in $^{12}\text{C}$



**Thomas Neff**

**International Workshop XLIII on Gross Properties  
of Nuclei and Nuclear Excitations**

**Hirschegg, Kleinwalsertal, Austria  
January 11-17, 2015**



# Overview



Realistic Effective Nucleon-Nucleon interaction:  
**Unitary Correlation Operator Method**

Many-Body Approach:  
**Fermionic Molecular Dynamics**

Application:

**${}^3\text{He}(\alpha, \gamma){}^7\text{Be}$  Radiative Capture**

**Microscopic Cluster Model for  ${}^{12}\text{C}$**

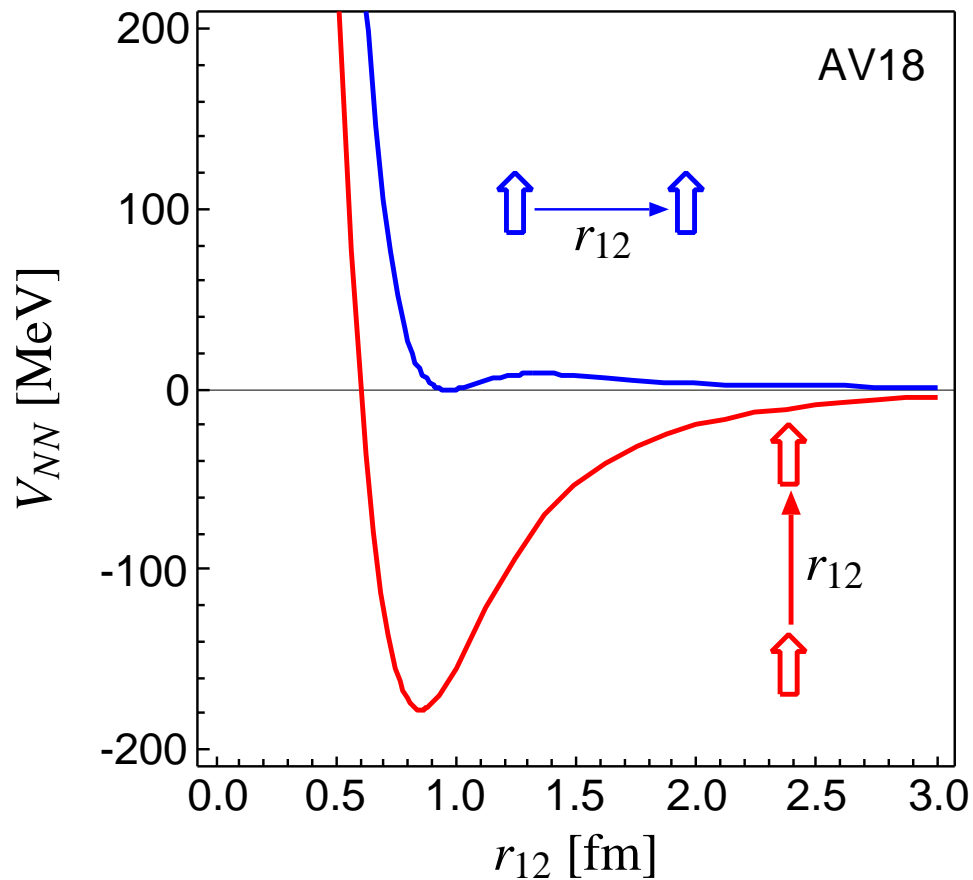
- **three  $\alpha$  and  ${}^8\text{Be}$ - $\alpha$  configurations**
- **Coulomb asymptotics: resonances and scattering states**

**FMD calculation for  ${}^{12}\text{C}$**

# Nuclear Force

Argonne V18 (T=0)

spins aligned parallel or perpendicular to the relative distance vector



- strong repulsive core: nucleons can not get closer than  $\approx 0.5$  fm

➔ **central correlations**

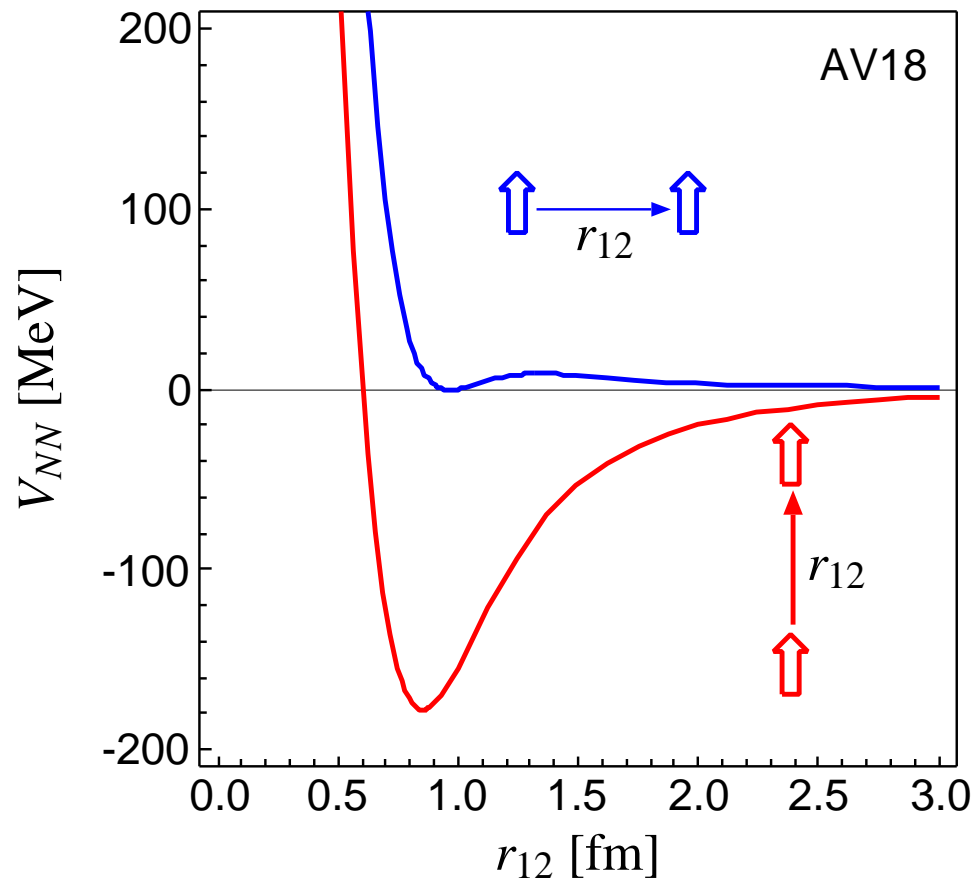
- strong dependence on the orientation of the spins due to the tensor force

➔ **tensor correlations**

# Nuclear Force

Argonne V18 (T=0)

spins aligned parallel or perpendicular to the relative distance vector



- strong repulsive core: nucleons can not get closer than  $\approx 0.5$  fm

➔ **central correlations**

- strong dependence on the orientation of the spins due to the tensor force

➔ **tensor correlations**

the nuclear force will induce **strong short-range correlations** in the nuclear wave function

- Central and Tensor Correlations

$$\tilde{\zeta} = \tilde{\zeta}_\Omega \tilde{\zeta}_r$$

$$\mathbf{p} = \mathbf{p}_r + \mathbf{p}_\Omega$$

$$\mathbf{p}_r = \frac{1}{2} \left\{ \frac{\mathbf{r}}{r} \left( \frac{\mathbf{r}}{r} \mathbf{p} \right) + \left( \mathbf{p} \frac{\mathbf{r}}{r} \right) \frac{\mathbf{r}}{r} \right\}, \quad \mathbf{p}_\Omega = \frac{1}{2r} \left\{ \mathbf{I} \times \frac{\mathbf{r}}{r} - \frac{\mathbf{r}}{r} \times \mathbf{I} \right\}$$

# Central and Tensor Correlations

$$\zeta = \zeta_\Omega \zeta_r$$

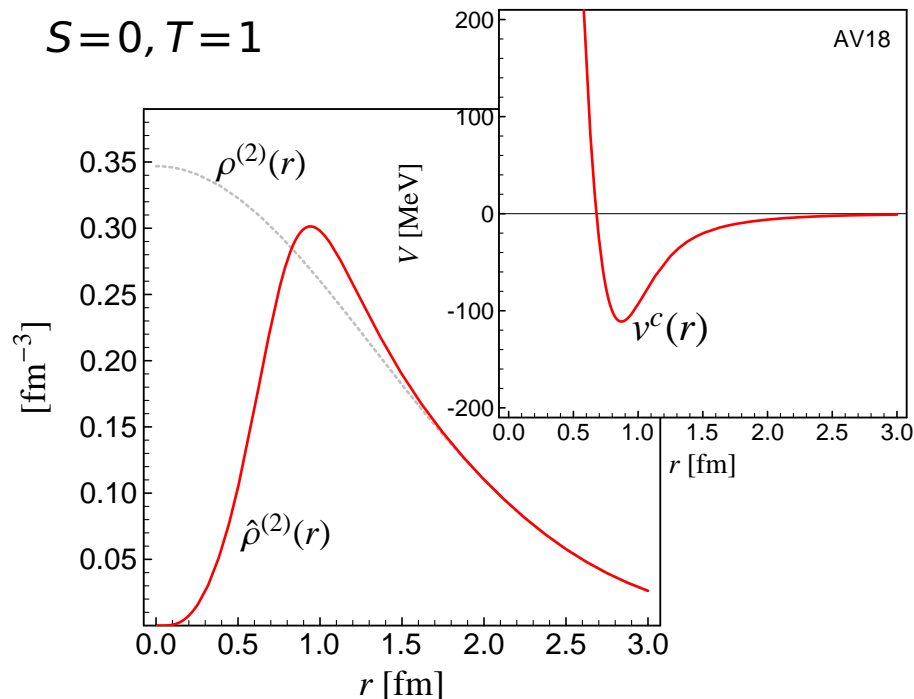
$$\mathbf{p} = \mathbf{p}_r + \mathbf{p}_\Omega$$

$$\mathbf{p}_r = \frac{1}{2} \left\{ \frac{\mathbf{r}}{r} (\mathbf{r} \cdot \mathbf{p}) + (\mathbf{p} \cdot \frac{\mathbf{r}}{r}) \frac{\mathbf{r}}{r} \right\}, \quad \mathbf{p}_\Omega = \frac{1}{2r} \left\{ \mathbf{l} \times \frac{\mathbf{r}}{r} - \frac{\mathbf{r}}{r} \times \mathbf{l} \right\}$$

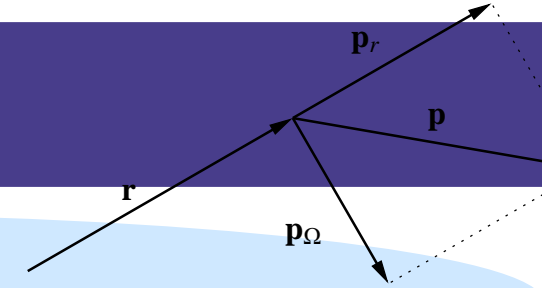
## Central Correlations

$$\zeta_r = \exp \left\{ -\frac{i}{2} \{ p_r s(r) + s(r) p_r \} \right\}$$

➔ probability density shifted out of the repulsive core



- UCOM
- Central and Tensor Correlations



$$\zeta = \zeta_\Omega \zeta_r$$

$$\mathbf{p} = \mathbf{p}_r + \mathbf{p}_\Omega$$

$$\mathbf{p}_r = \frac{1}{2} \left\{ \frac{\mathbf{r}}{r} (\mathbf{r} \cdot \mathbf{p}) + (\mathbf{p} \cdot \frac{\mathbf{r}}{r}) \frac{\mathbf{r}}{r} \right\}, \quad \mathbf{p}_\Omega = \frac{1}{2r} \left\{ \mathbf{l} \times \frac{\mathbf{r}}{r} - \frac{\mathbf{r}}{r} \times \mathbf{l} \right\}$$

### Central Correlations

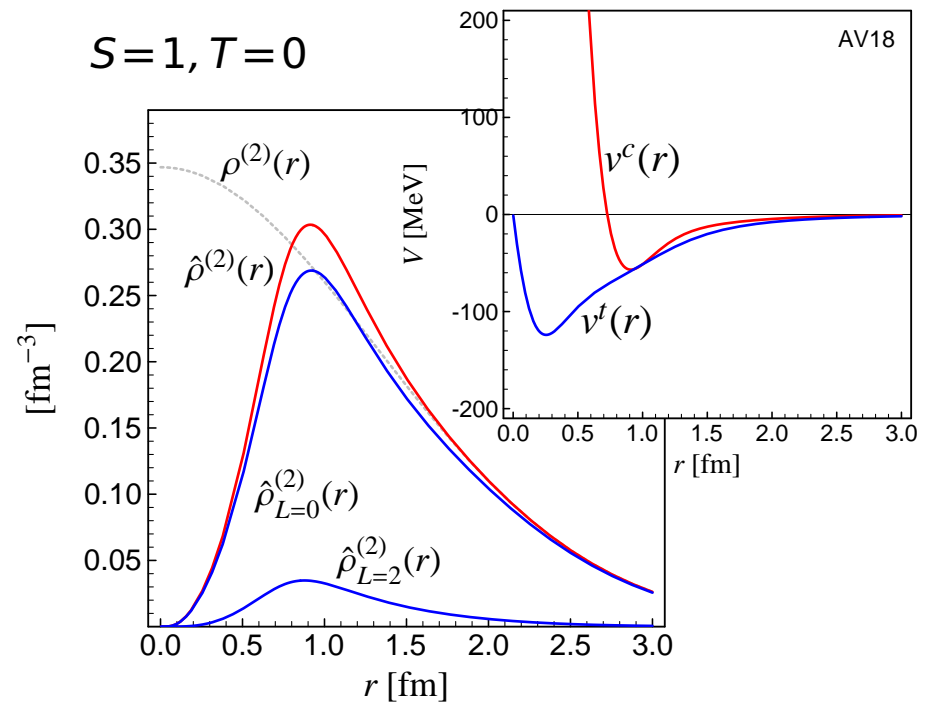
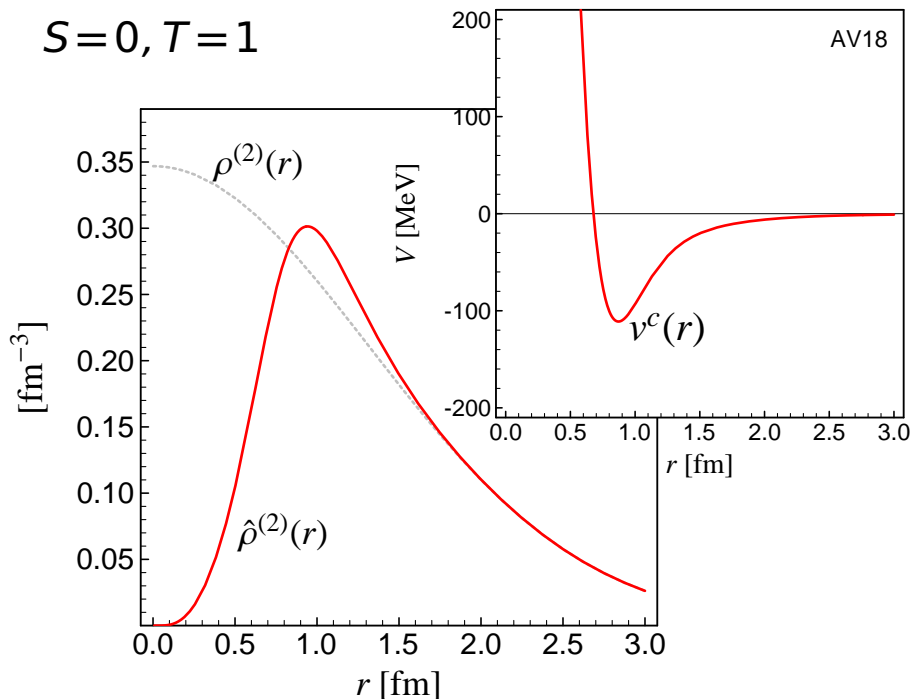
$$\zeta_r = \exp \left\{ -\frac{i}{2} \{ p_r s(r) + s(r) p_r \} \right\}$$

➔ probability density shifted out of the repulsive core

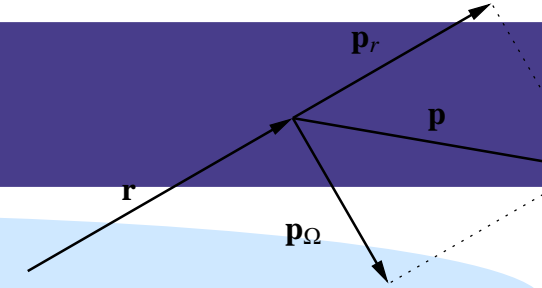
### Tensor Correlations

$$\zeta_\Omega = \exp \left\{ -i\theta(r) \left\{ \frac{3}{2} (\boldsymbol{\sigma}_1 \cdot \mathbf{p}_\Omega) (\boldsymbol{\sigma}_2 \cdot \mathbf{r}) + \frac{3}{2} (\boldsymbol{\sigma}_1 \cdot \mathbf{r}) (\boldsymbol{\sigma}_2 \cdot \mathbf{p}_\Omega) \right\} \right\}$$

➔ tensor force admixes other angular momenta



- UCOM
- Central and Tensor Correlations



$$\zeta = \zeta_\Omega \zeta_r$$

$$\mathbf{p} = \mathbf{p}_r + \mathbf{p}_\Omega$$

$$\mathbf{p}_r = \frac{1}{2} \left\{ \frac{\mathbf{r}}{r} (\mathbf{r} \cdot \mathbf{p}) + (\mathbf{p} \cdot \frac{\mathbf{r}}{r}) \frac{\mathbf{r}}{r} \right\}, \quad \mathbf{p}_\Omega = \frac{1}{2r} \left\{ \mathbf{I} \times \frac{\mathbf{r}}{r} - \frac{\mathbf{r}}{r} \times \mathbf{I} \right\}$$

### Central Correlations

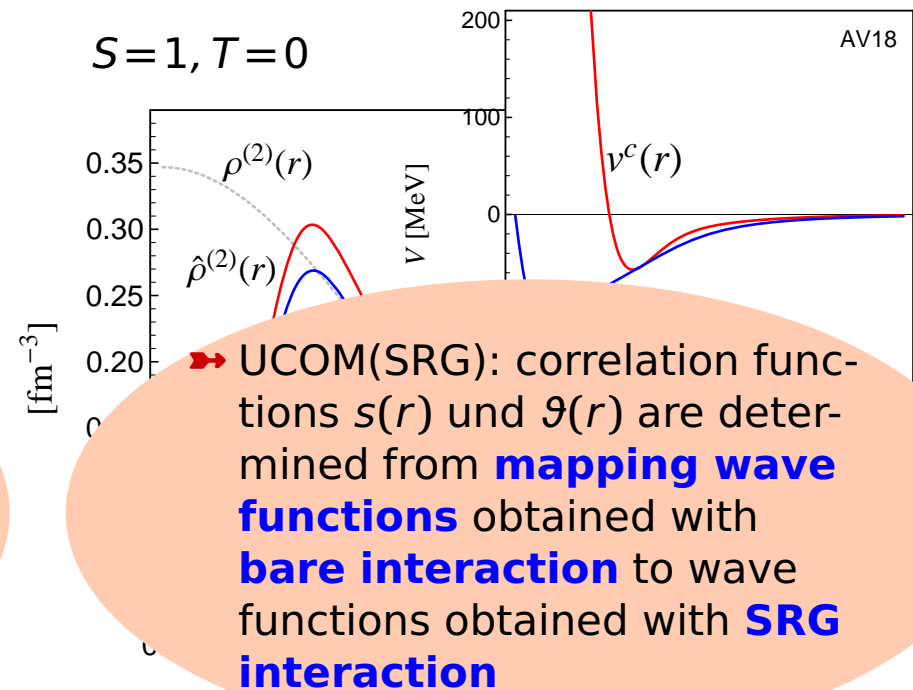
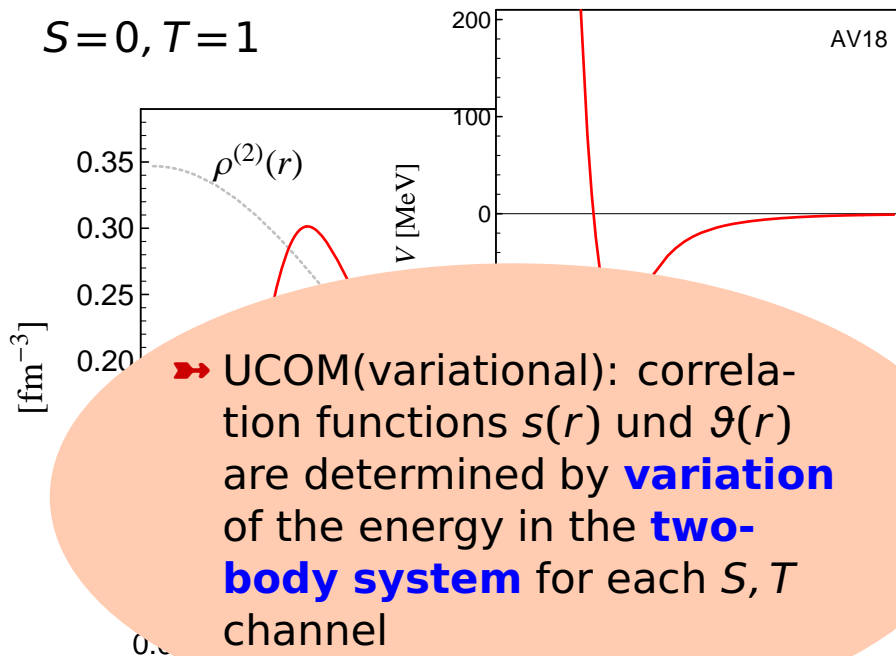
$$\zeta_r = \exp \left\{ -\frac{i}{2} \{ p_r s(r) + s(r) p_r \} \right\}$$

➔ probability density shifted out of the repulsive core

### Tensor Correlations

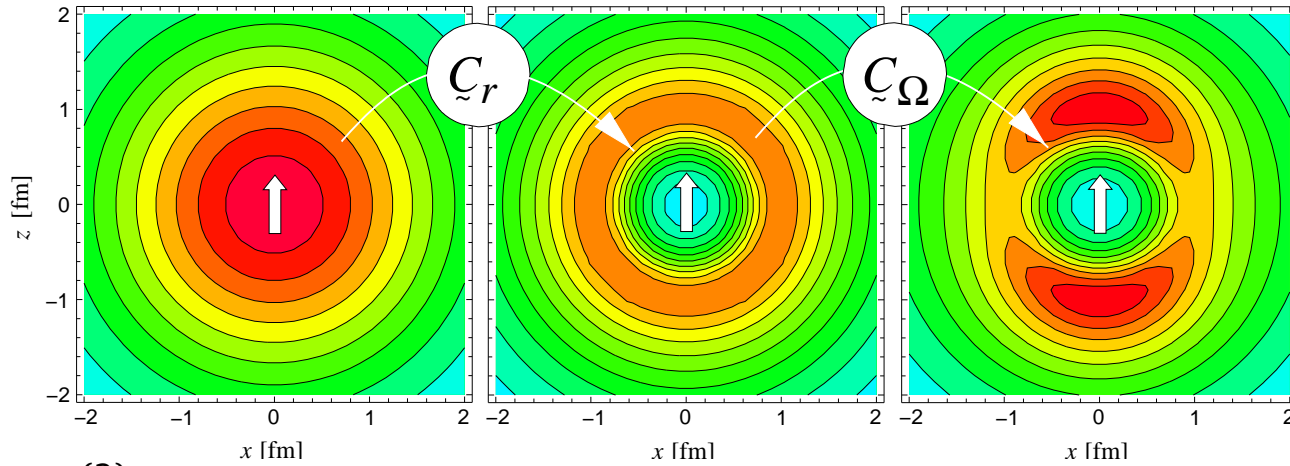
$$\zeta_\Omega = \exp \left\{ -i\vartheta(r) \left\{ \frac{3}{2} (\boldsymbol{\sigma}_1 \cdot \mathbf{p}_\Omega) (\boldsymbol{\sigma}_2 \cdot \mathbf{r}) + \frac{3}{2} (\boldsymbol{\sigma}_1 \cdot \mathbf{r}) (\boldsymbol{\sigma}_2 \cdot \mathbf{p}_\Omega) \right\} \right\}$$

➔ tensor force admixes other angular momenta





two-body densities



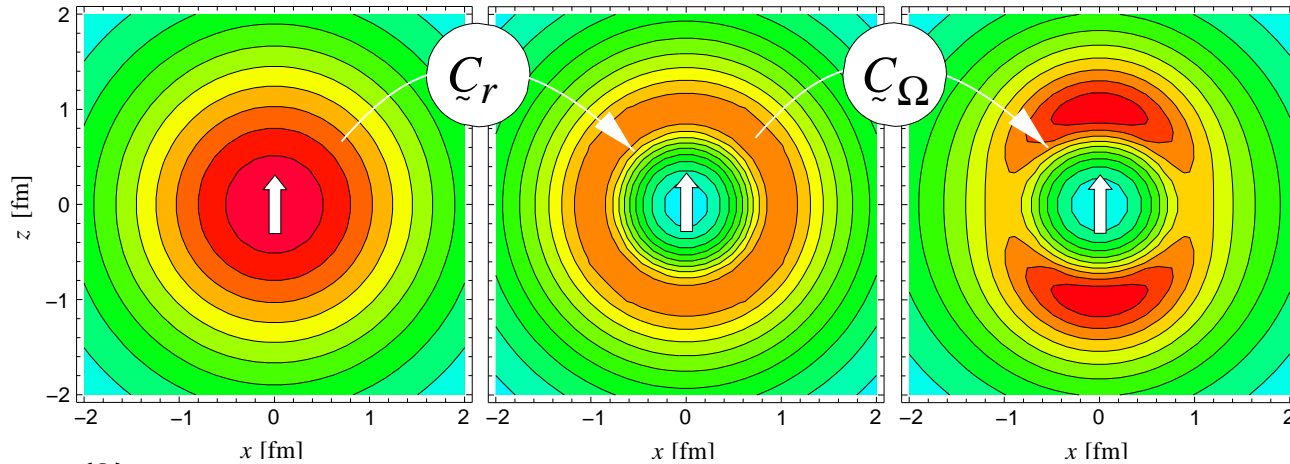
$$\rho_{S,T}^{(2)}(\mathbf{r}_1 - \mathbf{r}_2) \quad S = 1, M_S = 1, T = 0$$

**central correlator**  $\tilde{C}_r$   
shifts density out of  
the repulsive core

**tensor correlator**  $\tilde{C}_\Omega$   
aligns density with spin  
orientation

# Correlations and Energies

two-body densities

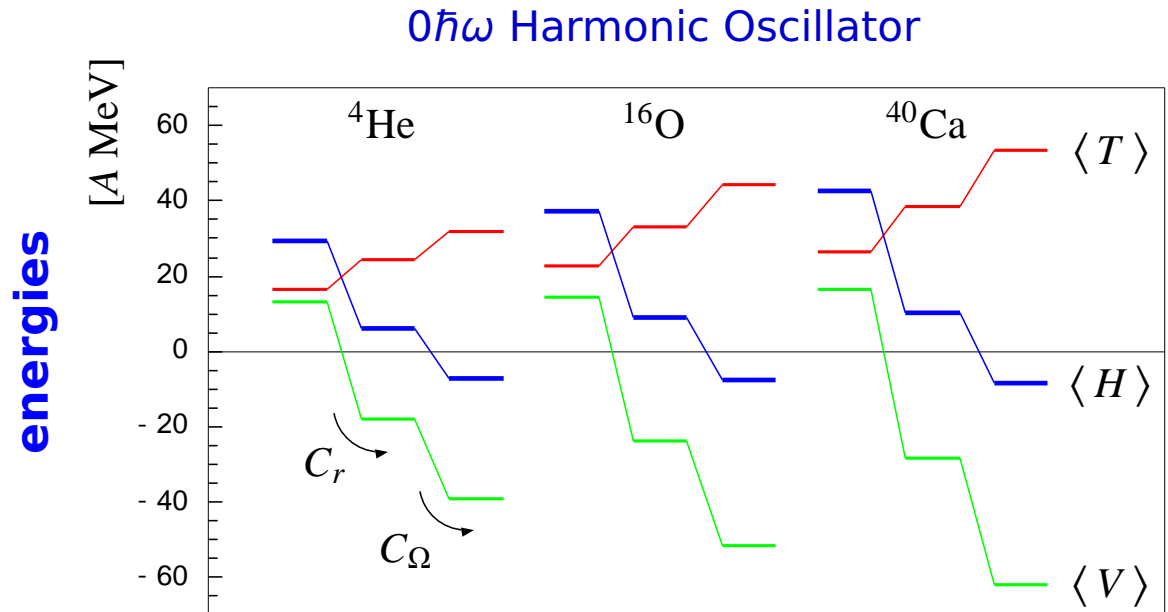


$$\rho_{S,T}^{(2)}(\mathbf{r}_1 - \mathbf{r}_2) \quad S = 1, M_S = 1, T = 0$$

**central correlator**  $\tilde{C}_r$   
shifts density out of  
the repulsive core

**tensor correlator**  $\tilde{C}_\Omega$   
aligns density with spin  
orientation

both central  
and tensor  
correlations are  
essential for  
binding



# Operator Representation of $V_{\text{UCOM}}$

$$\tilde{\zeta}^\dagger (\tilde{T} + \tilde{V}) \tilde{\zeta} = \tilde{T}$$

$$+ \sum_{ST} \hat{V}_c^{ST}(r) + \frac{1}{2} (p_r^2 \hat{V}_{p^2}^{ST}(r) + \hat{V}_{p^2}^{ST}(r) p_r^2) + \hat{V}_{l^2}^{ST}(r) \mathbf{l}^2$$

one-body kinetic energy

**central** potentials

$$+ \sum_T \hat{V}_{ls}^T(r) \mathbf{l} \cdot \mathbf{s} + \hat{V}_{l^2ls}^T(r) \mathbf{l}^2 \mathbf{l} \cdot \mathbf{s}$$

**spin-orbit** potentials

$$+ \sum_T \hat{V}_t^T(r) \mathcal{S}_{12}(\mathbf{r}, \mathbf{r}) + \hat{V}_{trp_\Omega}^T(r) p_r \mathcal{S}_{12}(\mathbf{r}, \mathbf{p}_\Omega) + \hat{V}_{tll}^T(r) \mathcal{S}_{12}(\mathbf{l}, \mathbf{l}) +$$

$$\hat{V}_{tp_\Omega p_\Omega}^T(r) \mathcal{S}_{12}(\mathbf{p}_\Omega, \mathbf{p}_\Omega) + \hat{V}_{l^2tp_\Omega p_\Omega}^T(r) \mathbf{l}^2 \mathcal{S}_{12}(\mathbf{p}_\Omega, \mathbf{p}_\Omega)$$

**tensor** potentials

bulk of tensor force mapped onto central part  
of correlated interaction  
tensor correlations also change the spin-orbit  
part of the interaction

## Fermionic

Slater determinant

$$|Q\rangle = \mathcal{A}\left(|q_1\rangle \otimes \cdots \otimes |q_A\rangle\right)$$

- antisymmetrized A-body state

## Fermionic

Slater determinant

$$|Q\rangle = \mathcal{A}\left(|q_1\rangle \otimes \cdots \otimes |q_A\rangle\right)$$

- antisymmetrized A-body state

## Molecular

single-particle states

$$\langle \mathbf{x} | q \rangle = \sum_i c_i \exp\left\{-\frac{(\mathbf{x} - \mathbf{b}_i)^2}{2a_i}\right\} \otimes |\chi_i^\uparrow, \chi_i^\downarrow\rangle \otimes |\xi\rangle$$

- Gaussian wave-packets in phase-space (complex parameter  $\mathbf{b}_i$  encodes mean position and mean momentum), spin is free, isospin is fixed
- width  $a_i$  is an independent variational parameter for each wave packet
- use one or two wave packets for each single particle state

# Fermionic Molecular Dynamics

## Fermionic

Slater determinant

$$|Q\rangle = \mathcal{A}\left(|q_1\rangle \otimes \cdots \otimes |q_A\rangle\right)$$

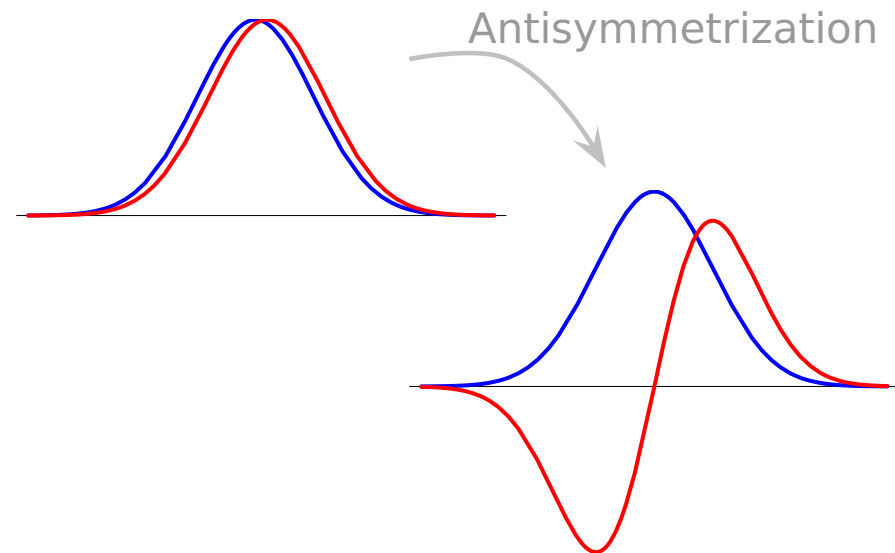
- antisymmetrized A-body state

## Molecular

single-particle states

$$\langle \mathbf{x} | q \rangle = \sum_i c_i \exp\left\{-\frac{(\mathbf{x} - \mathbf{b}_i)^2}{2a_i}\right\} \otimes |\chi_i^\uparrow, \chi_i^\downarrow\rangle \otimes |\xi\rangle$$

- Gaussian wave-packets in phase-space (complex parameter  $\mathbf{b}_i$  encodes mean position and mean momentum), spin is free, isospin is fixed
- width  $a_i$  is an independent variational parameter for each wave packet
- use one or two wave packets for each single particle state



# Fermionic Molecular Dynamics

## Fermionic

Slater determinant

$$|Q\rangle = \mathcal{A}\left(|q_1\rangle \otimes \cdots \otimes |q_A\rangle\right)$$

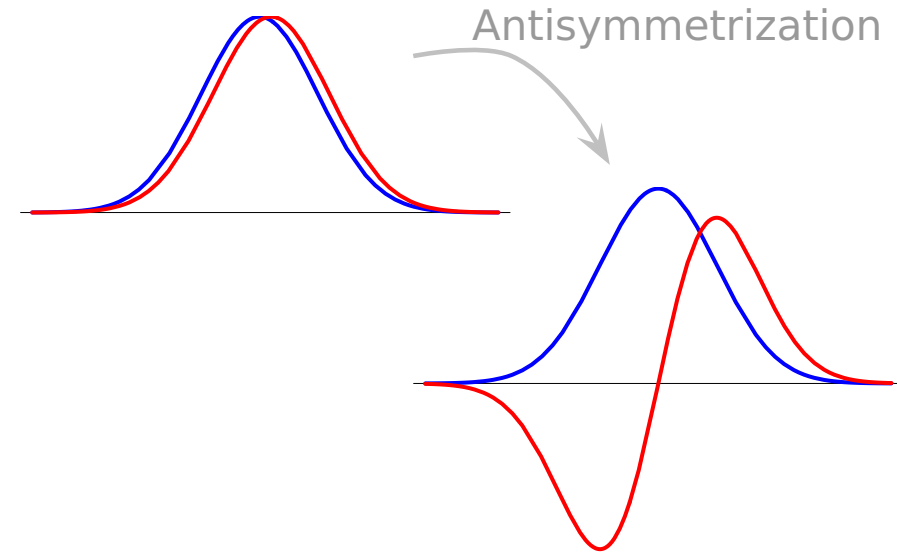
- antisymmetrized A-body state

## Molecular

single-particle states

$$\langle \mathbf{x} | q \rangle = \sum_i c_i \exp\left\{-\frac{(\mathbf{x} - \mathbf{b}_i)^2}{2a_i}\right\} \otimes |\chi_i^\uparrow, \chi_i^\downarrow\rangle \otimes |\xi\rangle$$

- Gaussian wave-packets in phase-space (complex parameter  $\mathbf{b}_i$  encodes mean position and mean momentum), spin is free, isospin is fixed
- width  $a_i$  is an independent variational parameter for each wave packet
- use one or two wave packets for each single particle state

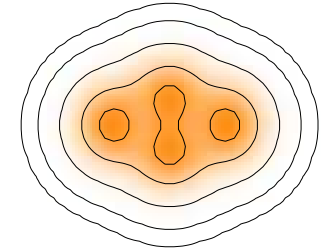


FMD basis contains  
HO shell model and  
microscopic cluster model  
as limiting cases

# Symmetries and Projection

## Breaking of symmetries

- Slater determinants  $|Q\rangle$  may break symmetries of the Hamiltonian with respect to parity, rotations and translations



## Projection

- Restore symmetries by projection

$$P_{\sim}^{\pi} = \frac{1}{2}(1 + \pi\Pi), \quad P_{\sim MK}^J = \frac{2J+1}{8\pi^2} \int d^3\Omega D_{MK}^{J*}(\Omega) R(\Omega), \quad P_{\sim}^{\mathbf{P}} = \frac{1}{(2\pi)^3} \int d^3X \exp\{-i(\tilde{\mathbf{P}} - \mathbf{P}) \cdot \mathbf{X}\}$$

## Multiconfiguration Mixing

- diagonalize** Hamiltonian in a set of projected intrinsic states  $\{|Q^{(a)}\rangle, a = 1, \dots, N\}$

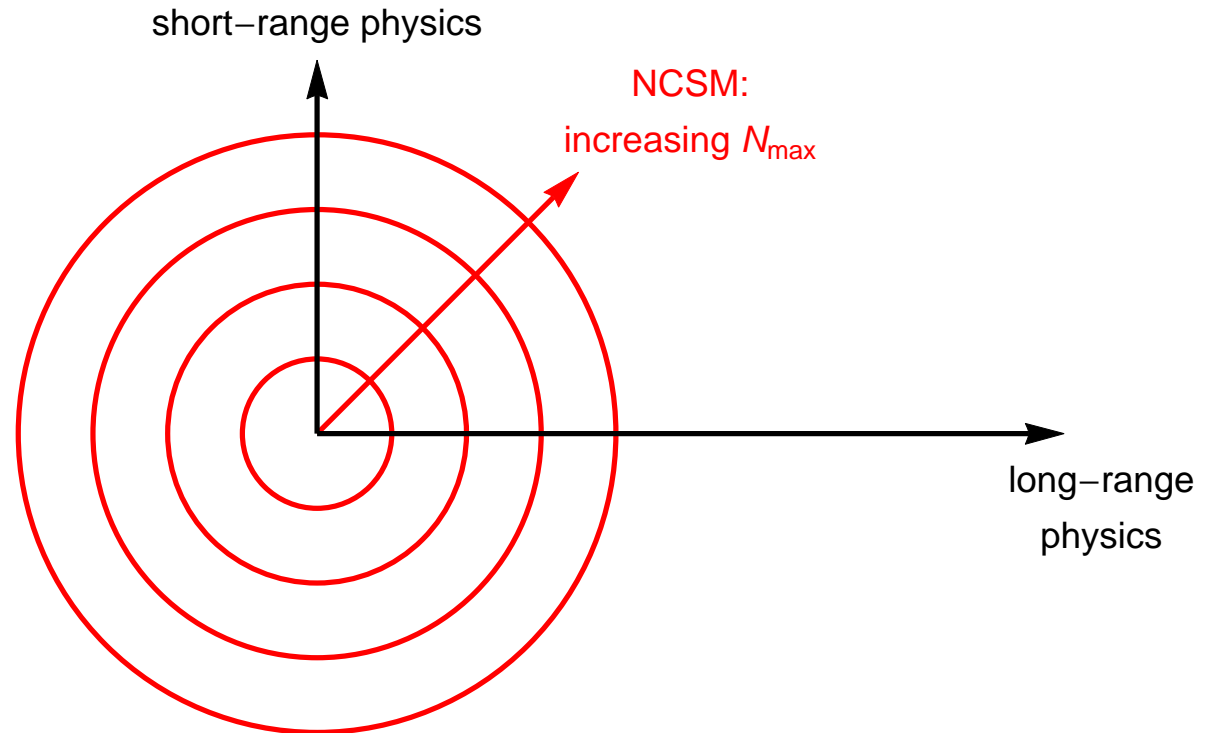
$$|\Psi; J^{\pi} M \alpha\rangle = \sum_{K\alpha} P_{\sim}^{\pi} P_{\sim MK}^J P_{\sim}^{\mathbf{P}=0} |Q^{(a)}\rangle c_{K\alpha}^{\alpha}$$

$$\sum_{K'b} \underbrace{\langle Q^{(a)} | H P_{\sim}^{\pi} P_{\sim KK'}^J P_{\sim}^{\mathbf{P}=0} | Q^{(b)} \rangle}_{\text{Hamiltonian kernel}} c_{K'b}^{\alpha} = E^{J^{\pi}\alpha} \sum_{K'b} \underbrace{\langle Q^{(a)} | P_{\sim}^{\pi} P_{\sim KK'}^J P_{\sim}^{\mathbf{P}=0} | Q^{(b)} \rangle}_{\text{norm kernel}} c_{K'b}^{\alpha}$$



- FMD

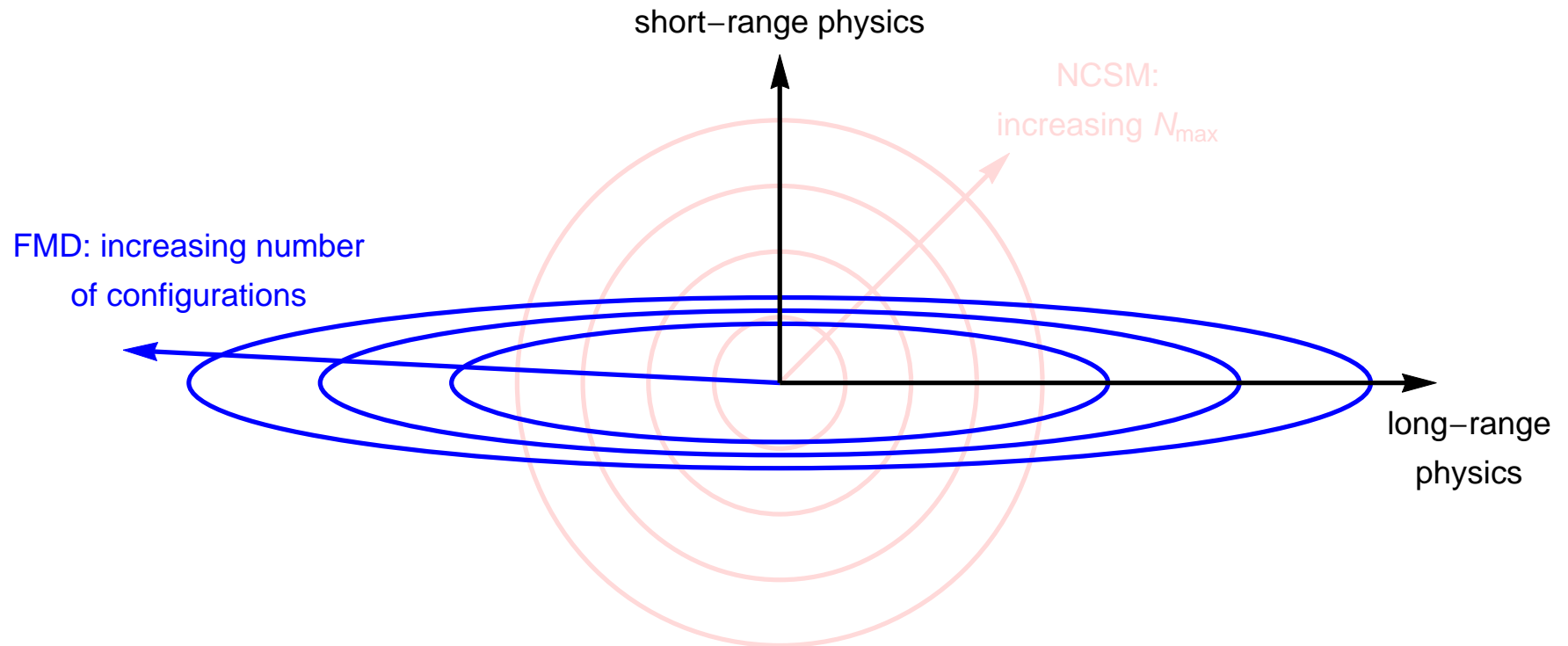
- **FMD vs NCSM model spaces**



- NCSM allows good description of short-range physics, but long-range behavior suffers from harmonic oscillator asymptotics

FMD

# FMD vs NCSM model spaces



- NCSM allows good description of short-range physics, but long-range behavior suffers from harmonic oscillator asymptotics
- FMD allows to describe long-range physics by superposition of localized cluster configurations, but limited in description of short-range physics

# ${}^3\text{He}(\alpha, \gamma){}^7\text{Be}$ radiative capture

one of the key reactions in the solar pp-chains



Effective Nucleon-Nucleon interaction:

**UCOM(SRG)**  $\alpha = 0.20 \text{ fm}^4 - \lambda \approx 1.5 \text{ fm}^{-1}$

Many-Body Approach:

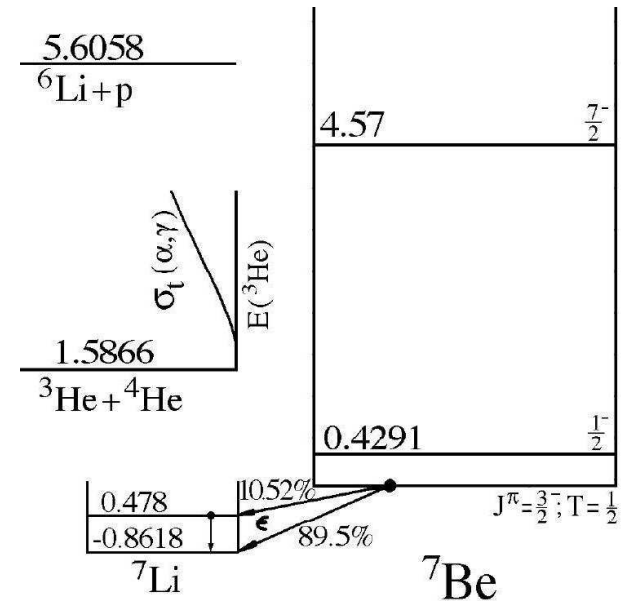
## Fermionic Molecular Dynamics

- Internal region: VAP configurations with radius constraint
- External region: Brink-type cluster configurations
- Matching to Coulomb solutions: Microscopic  $R$ -matrix method

Results:

- ${}^7\text{Be}$  bound and scattering states
- Astrophysical  $S$ -factor

Neff, Phys. Rev. Lett. 106, 042502 (2011)



${}^3\text{He}(\alpha, \gamma){}^7\text{Be}$

# FMD model space

## Frozen configurations

- antisymmetrized wave function built with  ${}^4\text{He}$  and  ${}^3\text{He}$  FMD clusters up to channel radius  $a=12$  fm

## Polarized configurations

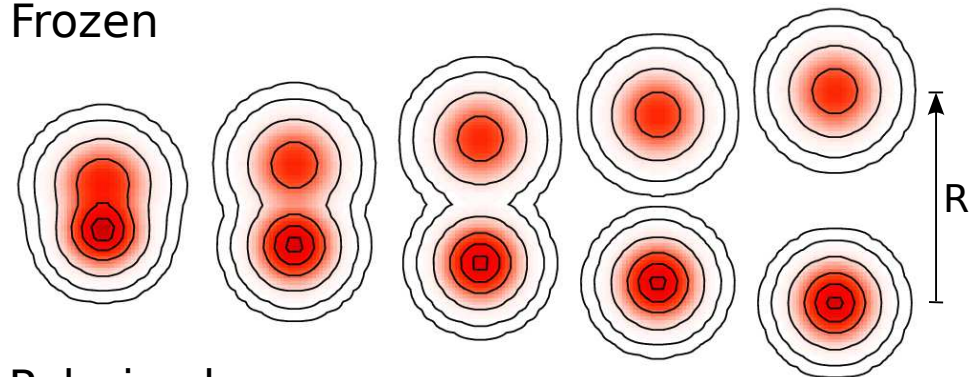
- FMD wave functions obtained by VAP on  $1/2^-$ ,  $3/2^-$ ,  $5/2^-$ ,  $7/2^-$  and  $1/2^+$ ,  $3/2^+$  and  $5/2^+$  combined with radius constraint in the interaction region

## Boundary conditions

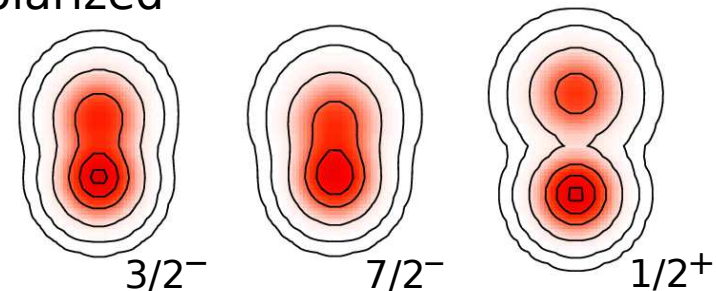
- Match relative motion of clusters at channel radius to Whittaker/Coulomb functions with the **microscopic R-matrix** method of the Brussels group

D. Baye, P.-H. Heenen, P. Descouvemont

Frozen



Polarized



# • $p$ -wave Bound and Scattering States

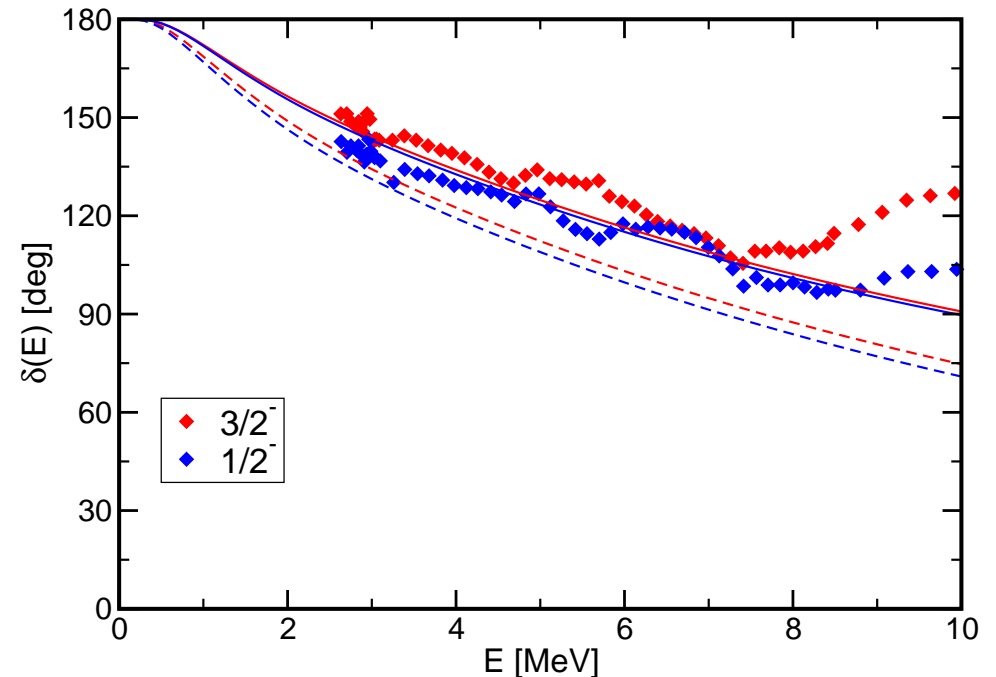
## Bound states

		Experiment	FMD
${}^7\text{Be}$	$E_{3/2-}$	-1.59 MeV	-1.49 MeV
	$E_{1/2-}$	-1.15 MeV	-1.31 MeV
	$r_{\text{ch}}$	2.647(17) fm	2.67 fm
	$Q$	-	-6.83 e fm <sup>2</sup>
${}^7\text{Li}$	$E_{3/2-}$	-2.467 MeV	-2.39 MeV
	$E_{1/2-}$	-1.989 MeV	-2.17 MeV
	$r_{\text{ch}}$	2.444(43) fm	2.46 fm
	$Q$	-4.00(3) e fm <sup>2</sup>	-3.91 e fm <sup>2</sup>

- centroid of bound state energies well described if polarized configurations included
- tail of wave functions tested by charge radii and quadrupole moments

## Phase shift analysis:

Spiger and Tombrello, PR **163**, 964 (1967)

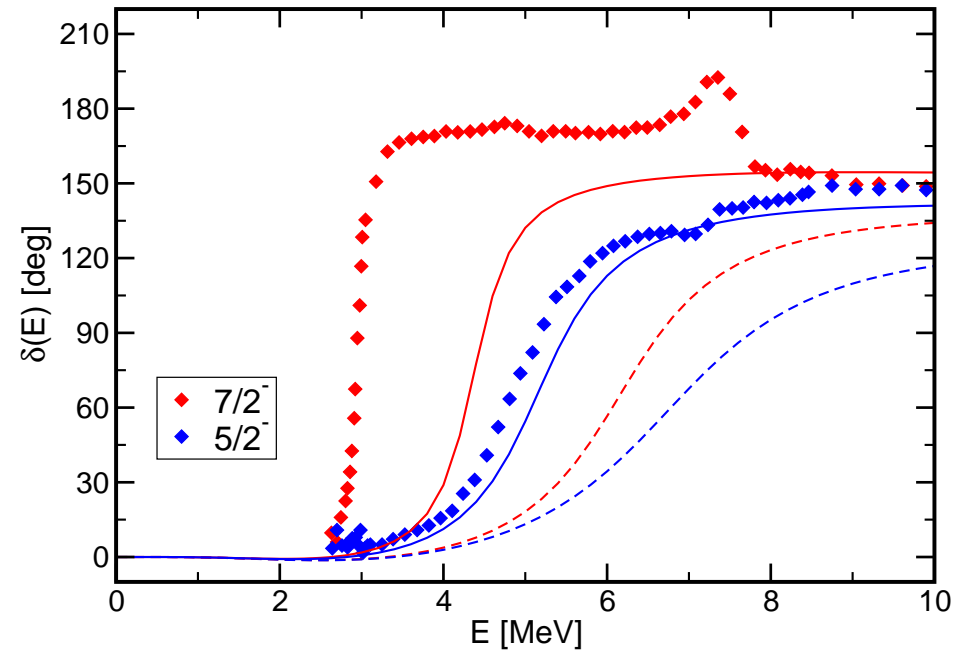
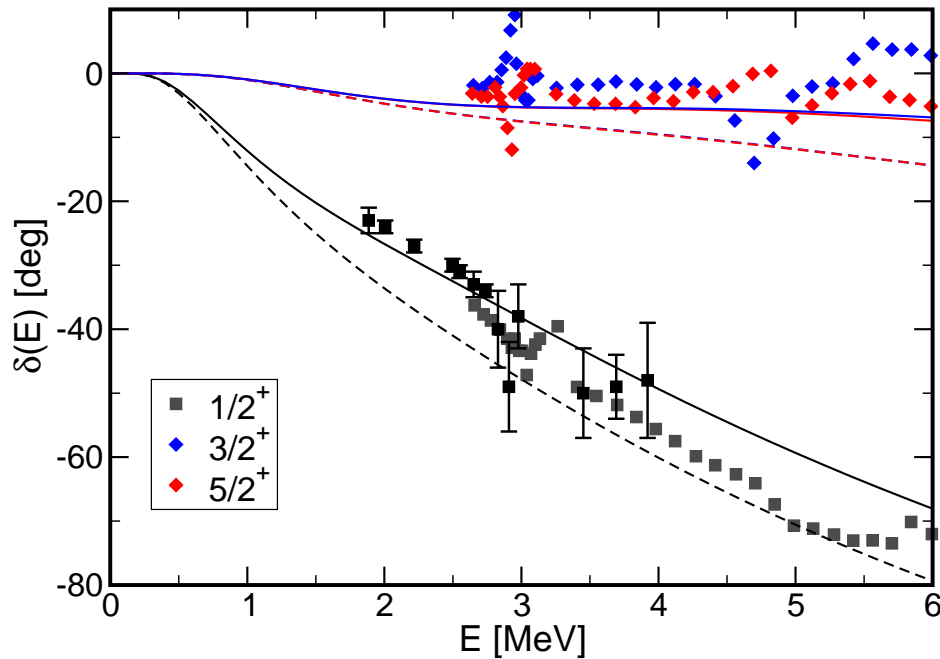


dashed lines – frozen configurations only  
solid lines – polarized configurations in interaction region included

- Scattering phase shifts well described, polarization effects important

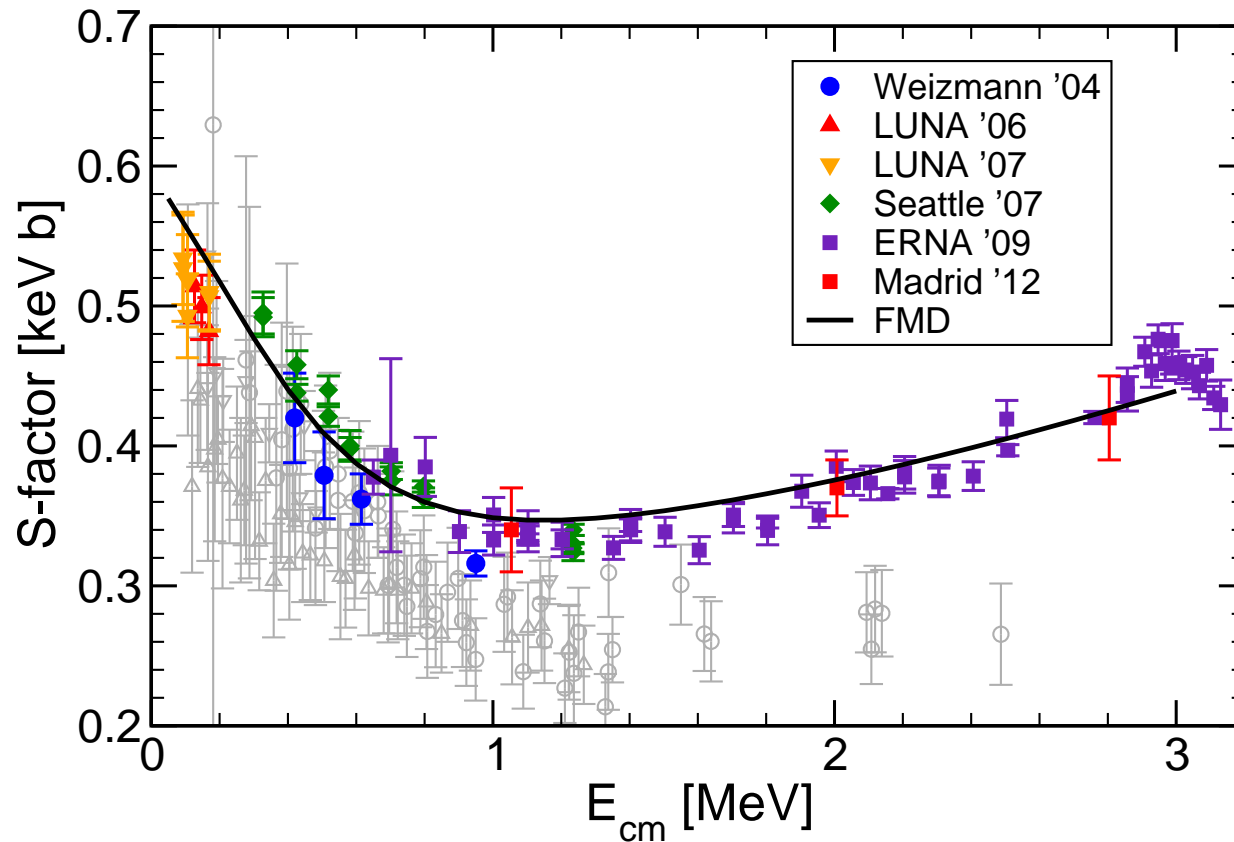
${}^3\text{He}(\alpha, \gamma){}^7\text{Be}$

# $s$ -, $d$ - and $f$ -wave Scattering States



dashed lines – frozen configurations only – solid lines – FMD configurations in interaction region included

- polarization effects important
- $s$ - and  $d$ -wave scattering phase shifts well described
- $f$ -wave splittings too small, additional spin-orbit strength from three-body forces expected



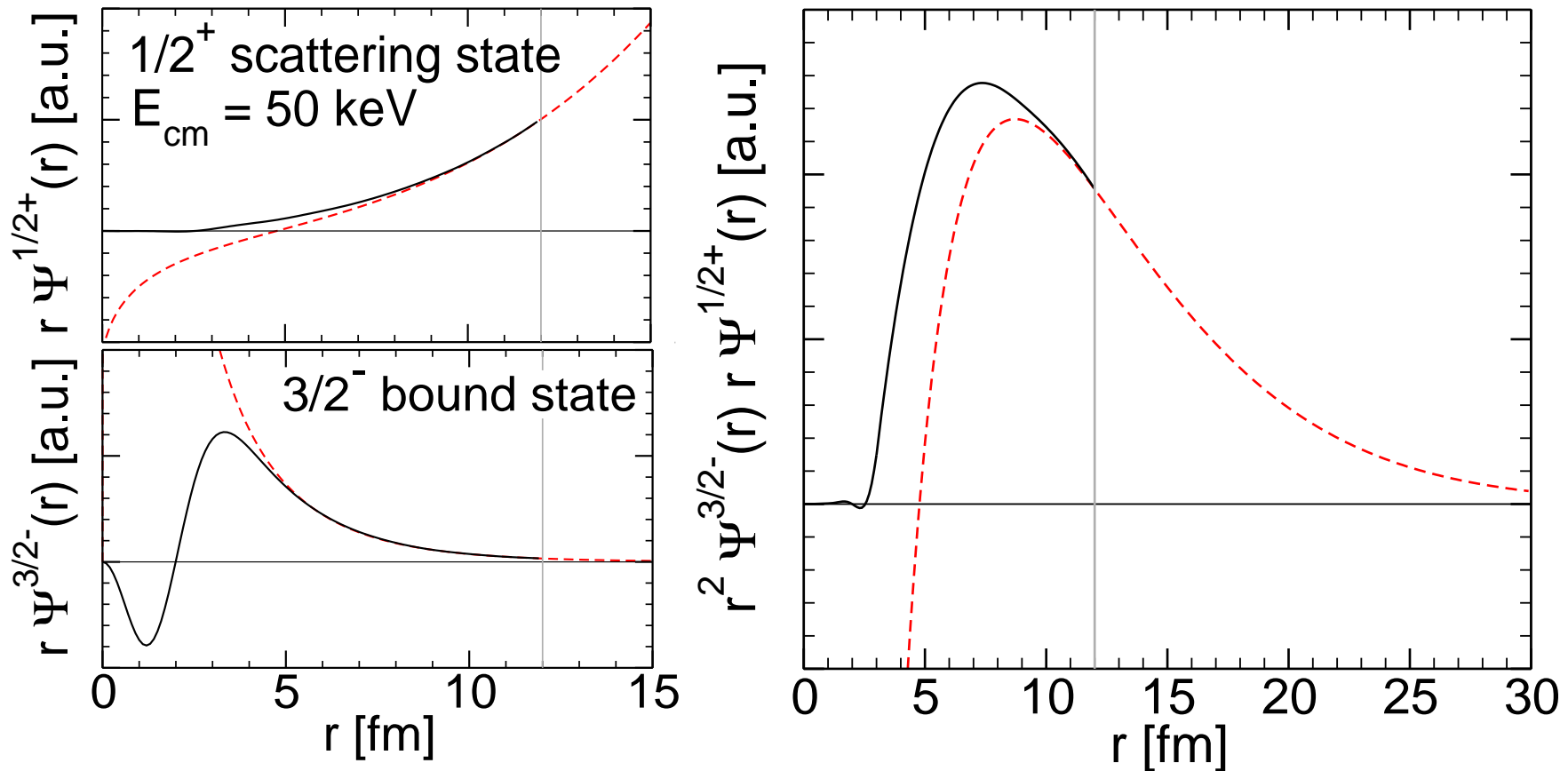
## S-factor:

$$S(E) = \sigma(E)E \exp\{2\pi\eta\}$$
$$\eta = \frac{\mu Z_1 Z_2 e^2}{k}$$

Nara Singh *et al.*, PRL **93**, 262503 (2004)  
Bemmerer *et al.*, PRL **97**, 122502 (2006)  
Confortola *et al.*, PRC **75**, 065803 (2007)  
Brown *et al.*, PRC **76**, 055801 (2007)  
Di Leva *et al.*, PRL **102**, 232502 (2009)

- dipole transitions from  $1/2^+$ ,  $3/2^+$ ,  $5/2^+$  scattering states into  $3/2^-$ ,  $1/2^-$  bound states
- FMD is the only model that describes well the energy dependence and normalization of new high quality data
- fully microscopic calculation, bound and scattering states are described consistently

# Overlap Functions and Dipole Matrixelements

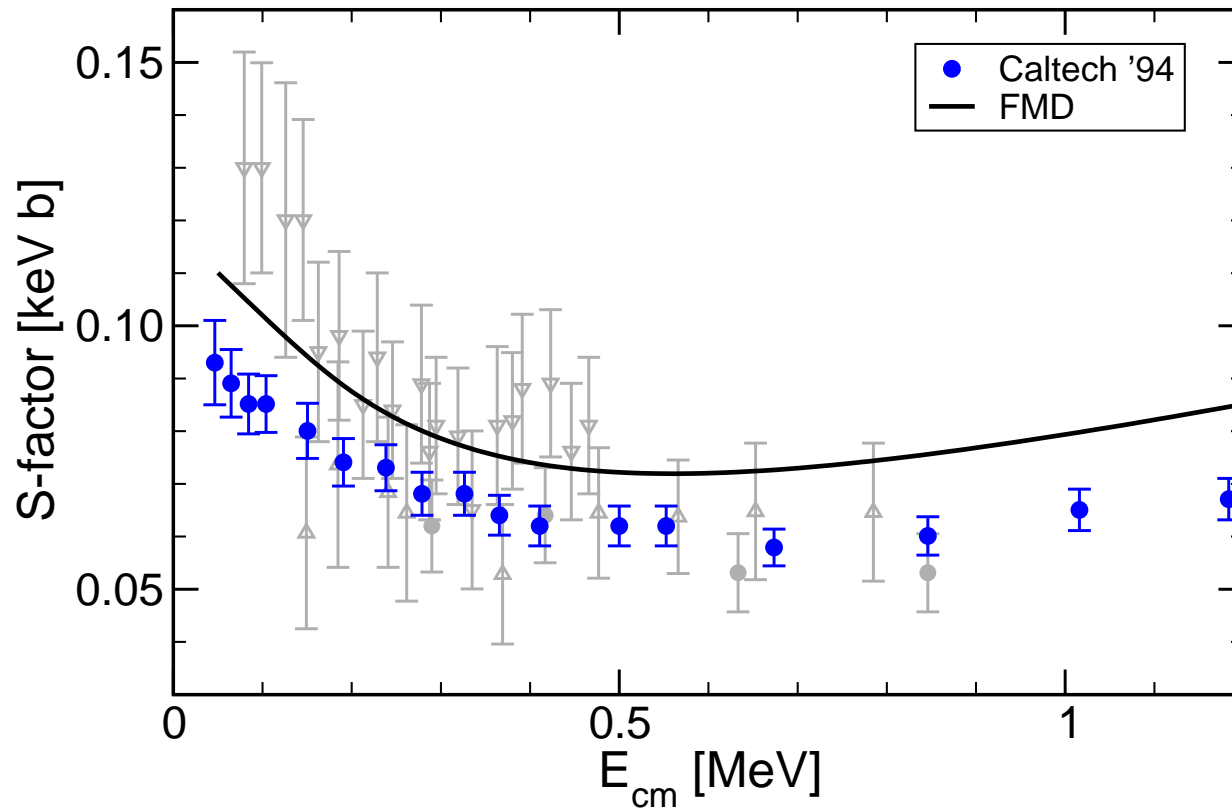


- Overlap functions from projection on RGM-cluster states
- Coulomb and Whittaker functions matched at channel radius  $a=12$  fm
- Dipole matrix elements calculated from overlap functions reproduce full calculation within 2%
- cross section depends significantly on internal part of wave function, description as an “external” capture is too simplified



${}^3\text{H}(\alpha, \gamma){}^7\text{Li}$

# S-Factor



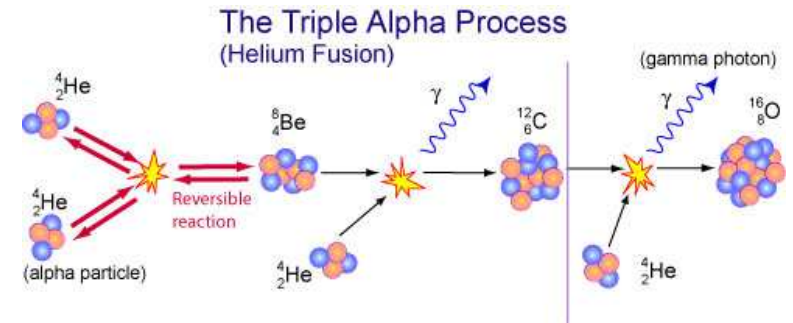
## S-factor:

$$S(E) = \sigma(E)E \exp\{2\pi\eta\}$$
$$\eta = \frac{\mu Z_1 Z_2 e^2}{k}$$

Brune *et al.*, PRC **50**, 2205 (1994)

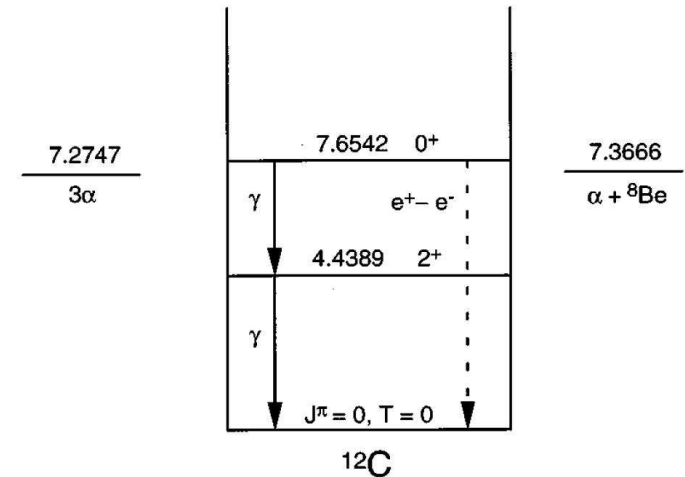
- isospin mirror reaction of  ${}^3\text{He}(\alpha, \gamma){}^7\text{Be}$
- ${}^7\text{Li}$  bound state properties and phase shifts well described
- ➔ FMD calculation describes energy dependence of Brune *et al.* data but cross section is larger by about 15%

# Cluster States in $^{12}\text{C}$



## Structure

- Is the Hoyle state a pure  $\alpha$ -cluster state ?
- Second  $2^+$  state  
Zimmermann *et al.*, Phys. Rev. Lett. 110, 152502 (2013)
- Second  $4^+$  state  
Freer *et al.*, Phys. Rev. C 83, 034314 (2011)
- Other states in the continuum  
Fynbo *et al.*, ...

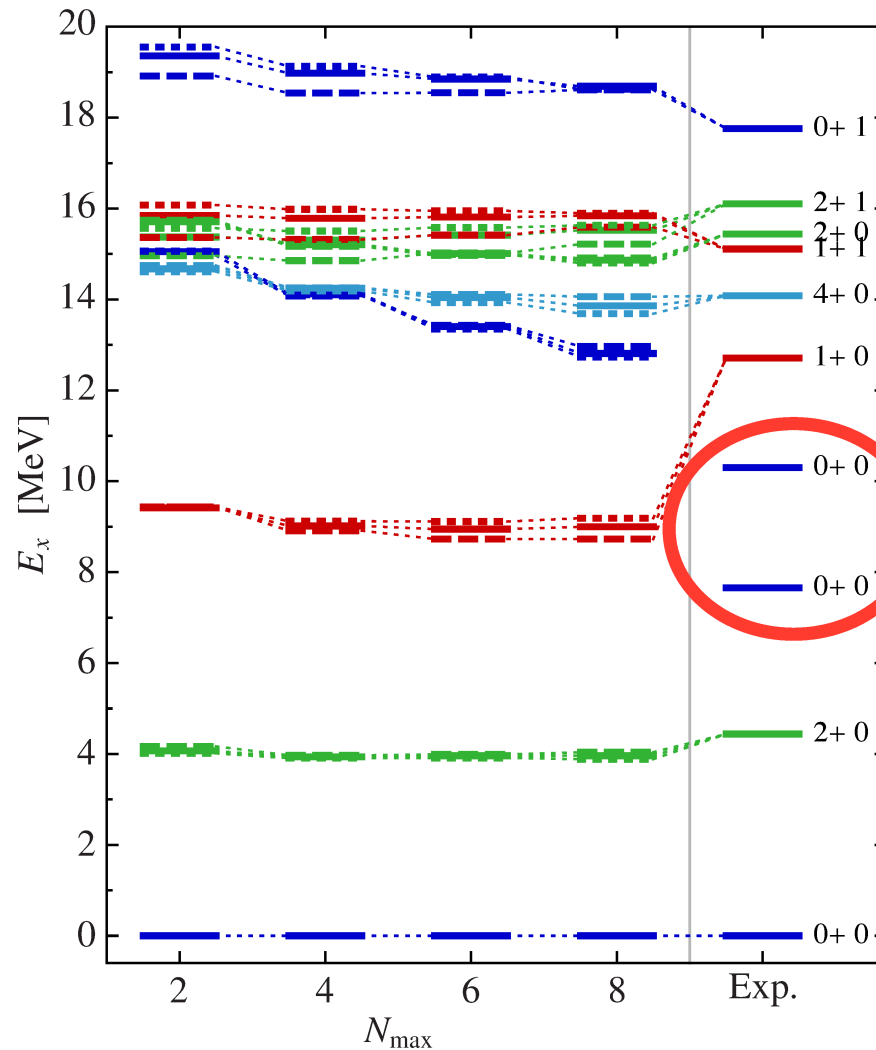


- ➔ Include continuum in the calculation!
- ➔ Compare FMD results to microscopic  $\alpha$ -cluster model

Neff, Feldmeier, arXiv:1409.3726

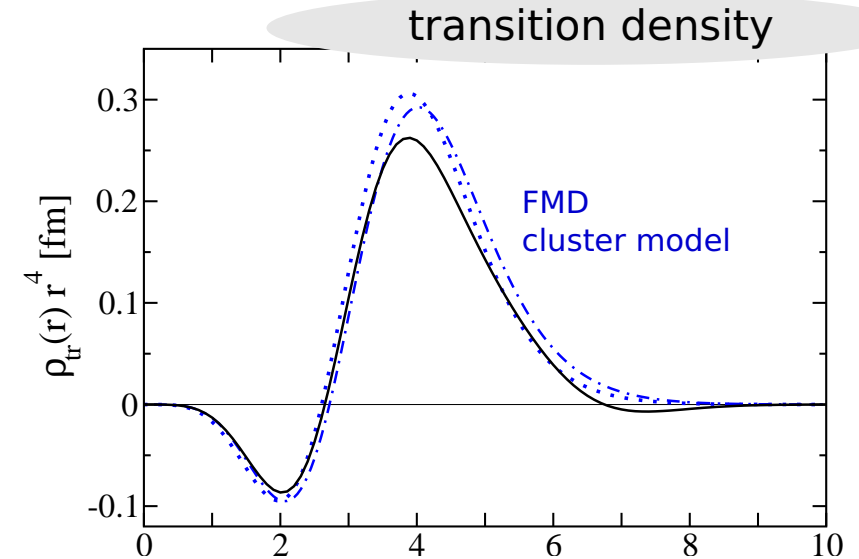
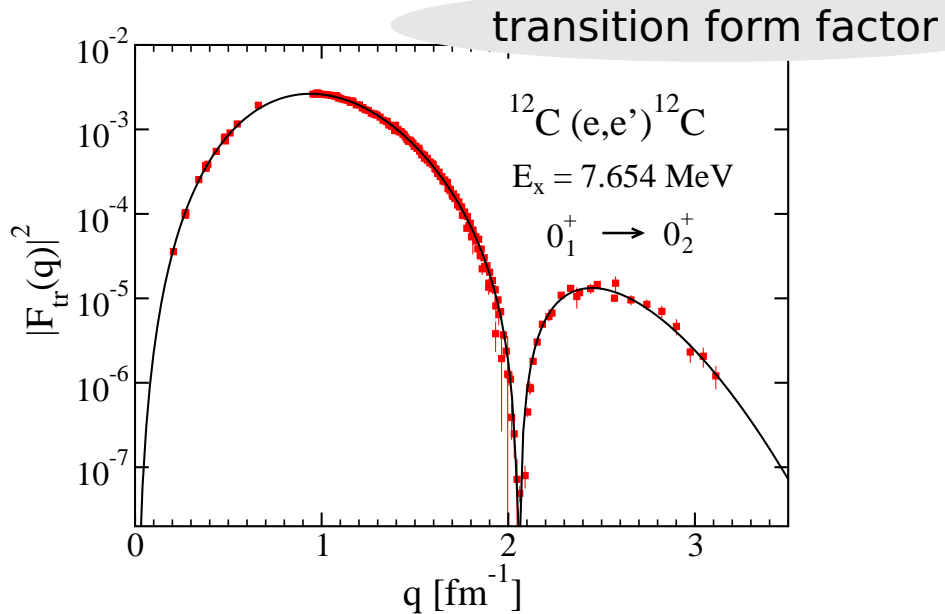
# Cluster States in $^{12}\text{C}$

## Cluster States in the NCSM ?

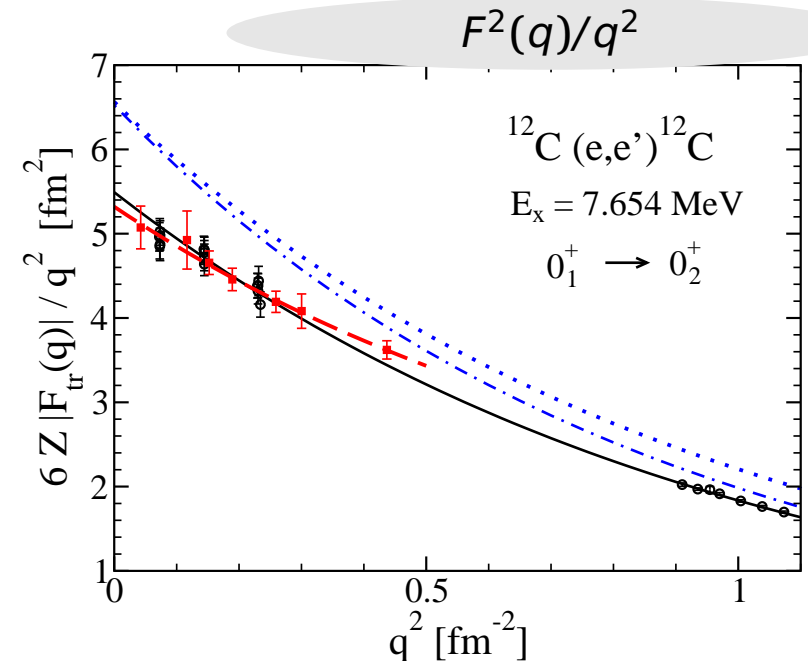


Hoyle state and other cluster states missing !

# Previous work on $^{12}\text{C}$ Monopole Matrix Element

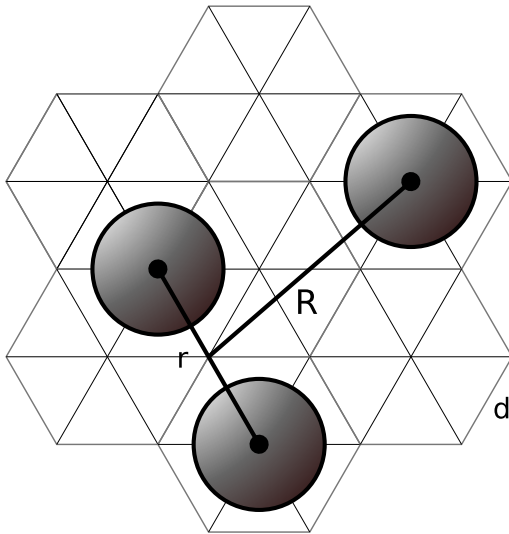


- model-independent self-consistent determination of transition form-factor/density in DWBA
- FMD and cluster model calculations in **bound-state approximation**



## Microscopic $\alpha$ -Cluster Model

# Model space in internal region



$$\rho^2 = \frac{1}{2} \mathbf{r}^2 + \frac{2}{3} \mathbf{R}^2$$

Hyperradius

## Model Space

- include all possible configurations on triangular grid ( $d = 1.4$  fm) up to a certain hyperradius  $\rho$
- no restriction on relative angular momenta

## Basis States

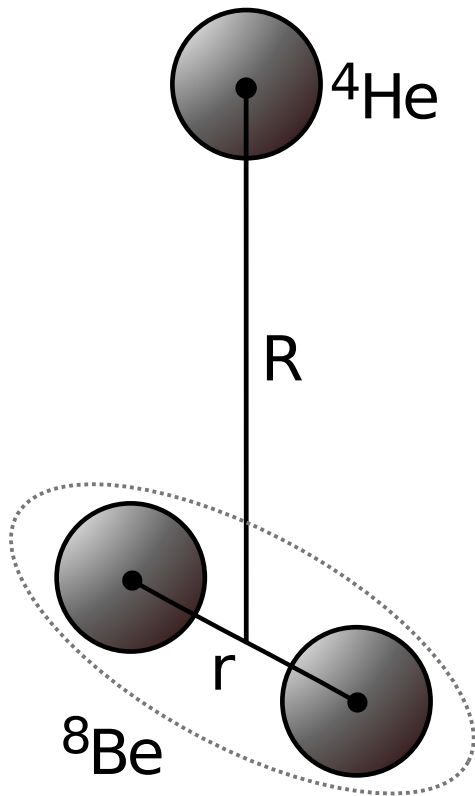
- Intrinsic states are projected on parity and angular momentum

$$|\Psi_{JMK\pi}^{3\alpha}(\mathbf{R}_1, \mathbf{R}_2, \mathbf{R}_3)\rangle = \sum_{\tilde{P} \tilde{M} \tilde{K} \tilde{A}} \tilde{P} \tilde{M} \tilde{K} \tilde{A} \left\{ |\Psi^{4\text{He}}(\mathbf{R}_1)\rangle \otimes |\Psi^{4\text{He}}(\mathbf{R}_2)\rangle \otimes |\Psi^{4\text{He}}(\mathbf{R}_3)\rangle \right\}$$

## Volkov Interaction

- simple central interaction
- parameters adjusted to give reasonable  $\alpha$  binding energy and radius,  $\alpha - \alpha$  scattering data, adjusted to reproduce  $^{12}\text{C}$  ground state energy

✗ only reasonable for  $^4\text{He}$ ,  $^8\text{Be}$  and  $^{12}\text{C}$  nuclei



## Model Space

- $^8\text{Be}$ - $^4\text{He}$  cluster configurations with generator coordinate  $R$
- $^8\text{Be}$  ground state ( $0_1^+$ ) and pseudo states ( $2_1^+$ ,  $0_2^+$ ,  $2_2^+$ ,  $4_1^+$ ) obtained by diagonalizing  $\alpha$ - $\alpha$  configurations up to  $r = 10$  fm

## Basis States

- $^{12}\text{C}$  basis states are obtained by **double projection**:  
Project first  $^8\text{Be}$

$$|\Psi_{IK}^{8\text{Be}}\rangle = \sum_i P_{\sim K0}^I \mathcal{A} \left\{ |\Psi^{4\text{He}}(-\frac{r_i}{2}\mathbf{e}_z)\rangle \otimes |\Psi^{4\text{He}}(+\frac{r_i}{2}\mathbf{e}_z)\rangle \right\} c_i^I$$

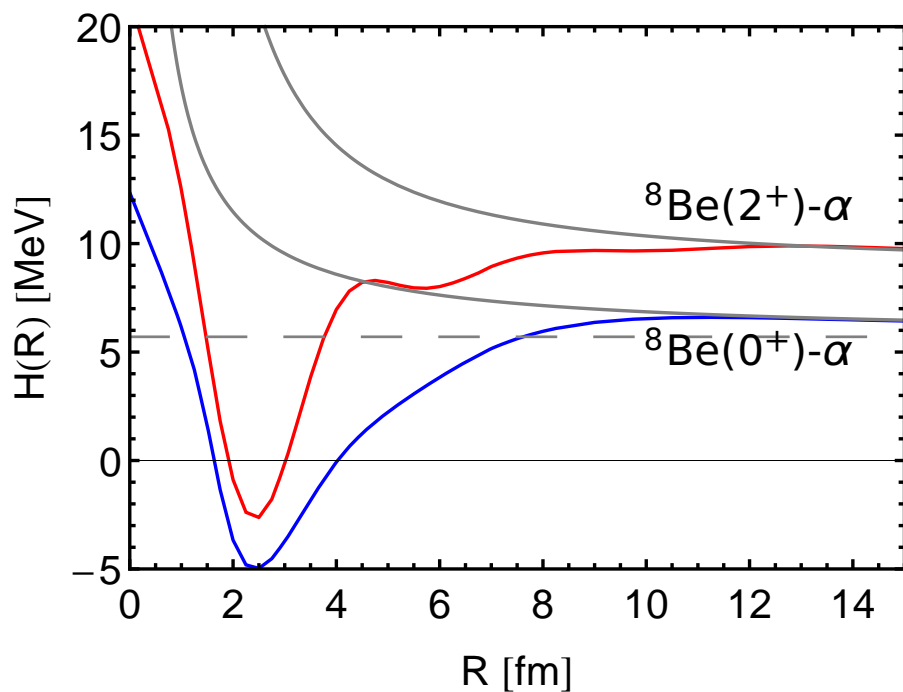
then the combined wave function

$$|\Psi_{IK;JM\pi}^{8\text{Be},4\text{He}}(R_j)\rangle = P_{\sim}^{\pi} P_{\sim MK}^J \mathcal{A} \left\{ |\Psi_{IK}^{8\text{Be}}(-\frac{R_j}{3}\mathbf{e}_z)\rangle \otimes |\Psi^{4\text{He}}(+\frac{2R_j}{3}\mathbf{e}_z)\rangle \right\}$$

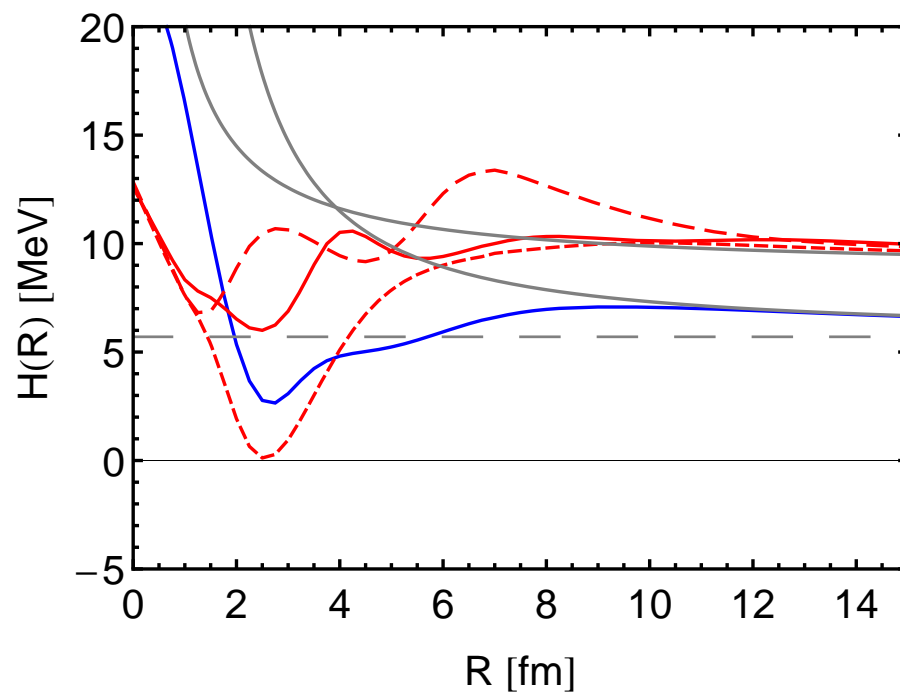
- will allow to match to Coulomb asymptotics

- Microscopic  $\alpha$ -Cluster Model
- $^8\text{Be}-\alpha$  Energy Surfaces

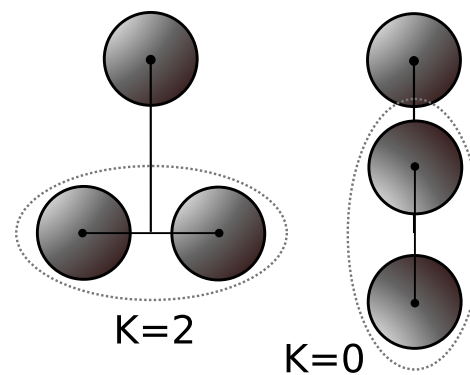
$J^\pi = 0^+$



$J^\pi = 2^+$



- energy surfaces contain localization energy for relative motion of  $^8\text{Be}$  and  $\alpha$
- $2^+$  energy surface depends strongly on orientation of  $^8\text{Be}$   $2^+$  state:  $K = 2$  most attractive



## Microscopic $\alpha$ -Cluster Model

# Bound state approximation – Convergence ?

	$\rho < 6$ fm	$\rho < 6$ fm, $R < 9$ fm	$\rho < 6$ fm, $R < 12$ fm	$\rho < 6$ fm, $R < 15$ fm	Experiment	
$E(0_1^+)$	-89.63	-89.64	-89.64	-89.64	-92.16	
$E^*(2_1^+)$	2.53	2.54	2.54	2.54	4.44	
$E^*(0_2^+), \Gamma_\alpha(0_2^+)$	8.53	7.82	7.78	7.76	$7.65, (8.5 \pm 1.0)10^{-6}$	
$E^*(2_2^+), \Gamma_\alpha(2_2^+)$	10.11	9.18	9.08	8.93	$10.13(5), 2.08^{+0.33}_{-0.26}$	[3]
$r_{\text{charge}}(0_1^+)$	2.53	2.53	2.53	2.53	2.47(2)	
$r(0_1^+)$	2.39	2.39	2.39	2.39	–	
$r(0_2^+)$	3.21	3.68	3.78	3.89	–	
$B(E2, 2_1^+ \rightarrow 0_1^+)$	9.03	9.12	9.08	9.08	7.6(4)	
$M(E0, 0_1^+ \rightarrow 0_2^+)$	7.20	6.55	6.40	6.27	5.47(9)	[2]
$B(E2, 2_2^+ \rightarrow 0_1^+)$	3.65	2.48	2.09	1.33	$1.57^{+0.14}_{-0.11}$	[3]

- properties of resonances (Hoyle state and second  $2^+$  state) can not be determined in bound state approximation in an unambiguous way

[1] Ajzenberg-Selove, Nuc. Phys. **A506**, 1 (1990)

[2] Chernykh et al., Phys. Rev. Lett. **105**, 022501 (2010)

[3] Zimmermann et al., Phys. Rev. Lett. **110**, 152502 (2013); H. Weller, *private communication*



- Microscopic  $\alpha$ -cluster model

- **Matching to Coulomb asymptotics**

## Model Space

- Internal region: 3- $\alpha$  configurations on a grid
- External region:  ${}^8\text{Be}(0^+, 2^+, 4^+)$ - $\alpha$  configurations
- Asymptotically: only Coulomb interaction between  ${}^8\text{Be}$  and  ${}^4\text{He}$  clusters

## GCM basis state expressed in RGM basis

- Microscopic GCM wave functions are functions of single-particle coordinates: internal wave functions of cluster, the relative motion of the clusters and the total center-of-mass motion are entangled
- Write GCM basis state in external region with RGM basis states

$$|\Psi_{IK;JM\pi}^{8\text{Be},4\text{He}}(R_j)\rangle = \sum_L \left\langle \begin{matrix} I & L \\ K & 0 \end{matrix} \middle| \begin{matrix} J \\ K \end{matrix} \right\rangle \int drr^2 \Gamma_L(R_j; r) |\Phi_{(IL)JM\pi}^{8\text{Be},4\text{He}}(r)\rangle \otimes |\Phi^{\text{cm}}\rangle$$

with  $(\pi = (-1)^L)$

$$\langle \boldsymbol{\rho}, \xi_a, \xi_b | \Phi_{(IL)JM\pi}^{8\text{Be},4\text{He}}(r) \rangle = \sum_{M_I, M_L} \left\langle \begin{matrix} I & L \\ M_I & M_L \end{matrix} \middle| \begin{matrix} J \\ M \end{matrix} \right\rangle \mathcal{A} \left\{ \frac{\delta(\rho - r)}{r^2} \Phi_{IM_I}^{8\text{Be}}(\xi_a) \Phi^{4\text{He}}(\xi_b) Y_{LM_L}(\hat{\rho}) \right\}$$

- asymptotically RGM states have good channel spin  $I$  and orbital angular momentum  $L$

- Microscopic  $\alpha$ -cluster model

- **Matching to Coulomb asymptotics**

## RGM norm kernel and Overlap functions

- RGM norm kernel reflects effects of antisymmetrization, channel  $c = (IL)J$

$$N_{c,c'}(r, r') = \langle \Phi_c(r) | \Phi_{c'}(r') \rangle \xrightarrow{r, r' \rightarrow \infty} \delta_{cc'} \frac{\delta(r - r')}{rr'}$$

- Overlap functions can be interpreted as wave functions for point-like clusters

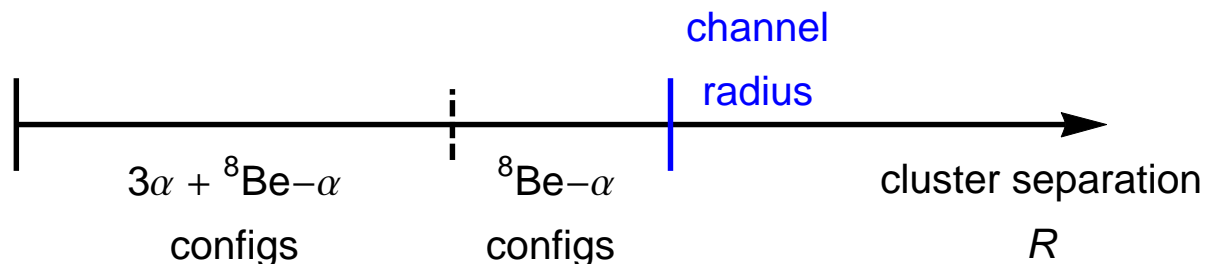
$$\psi_c(r) = \int dr' r'^2 N_{c,c'}^{-1/2}(r, r') \langle \Phi_{c'}(r') | \Psi \rangle$$

## Matching to the asymptotic solution

- Use using multichannel microscopic  $R$ -matrix approach

Descouvemont, Baye, Phys. Rept. 73, 036301 (2010)

- Check that results are independent from channel radius: used  $a = 16.5$  fm here



- Microscopic  $\alpha$ -cluster model
- **Matching to Coulomb asymptotics**

## Bound states

- Whittaker functions

$$\psi_c(r) = A_c \frac{1}{r} W_{-\eta_c, L_c + 1/2}(2\kappa_c r), \quad \kappa_c = \sqrt{-2\mu(E - E_c)}$$

## Resonances

- purely outgoing Coulomb,  $k$  complex

$$\psi_c(r) = A_c \frac{1}{r} O_{L_c}(\eta_c, k_c r), \quad k_c = \sqrt{2\mu(E - E_c)}$$

## Scattering states

- in- and outgoing Coulomb (incoming channel  $c_0$ )

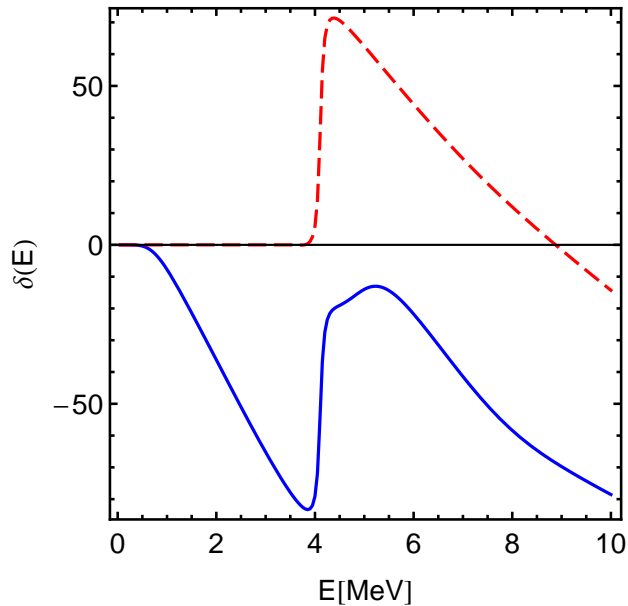
$$\psi_c(r) = \frac{1}{r} \{ \delta_{L_c, L_0} I_{L_c}(\eta_c, k_c r) - S_{c, c_0} O_{L_c}(\eta_c, k_c r) \}, \quad k_c = \sqrt{2\mu(E - E_c)}$$

- Diagonal phase shifts and inelasticity parameters:  $S_{cc} = \eta_c \exp\{2i\delta_c\}$
- Eigenphases:  $S = U^{-1} D U, D_{\alpha\alpha} = \exp\{2i\delta_\alpha\}$

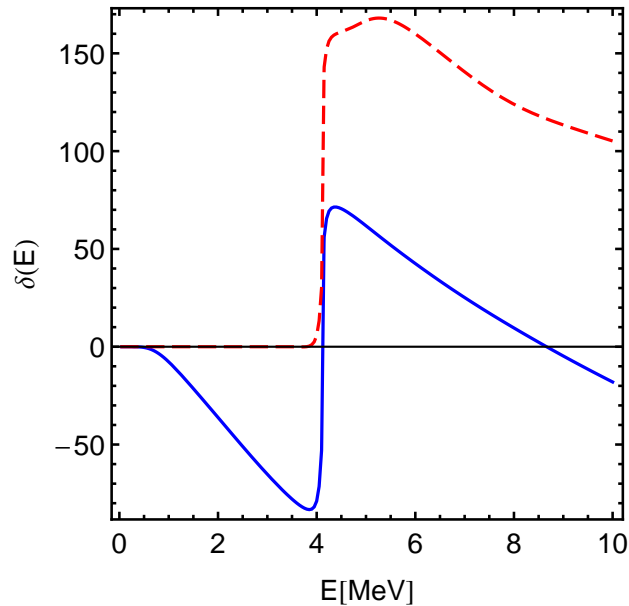
# Cluster Model: ${}^8\text{Be}(0_1^+, 2_1^+) - \alpha$ Continuum

## $0^+$ Phase shifts

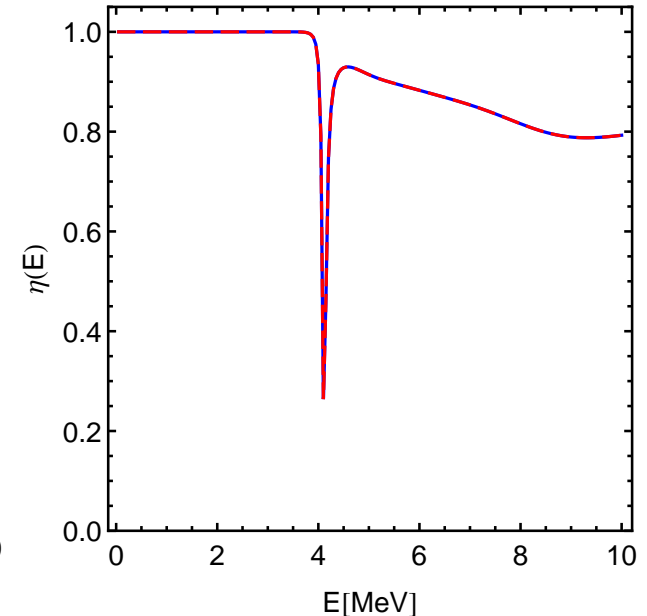
Eigenphaseshifts



Phaseshifts



Inelasticities



Gamow states

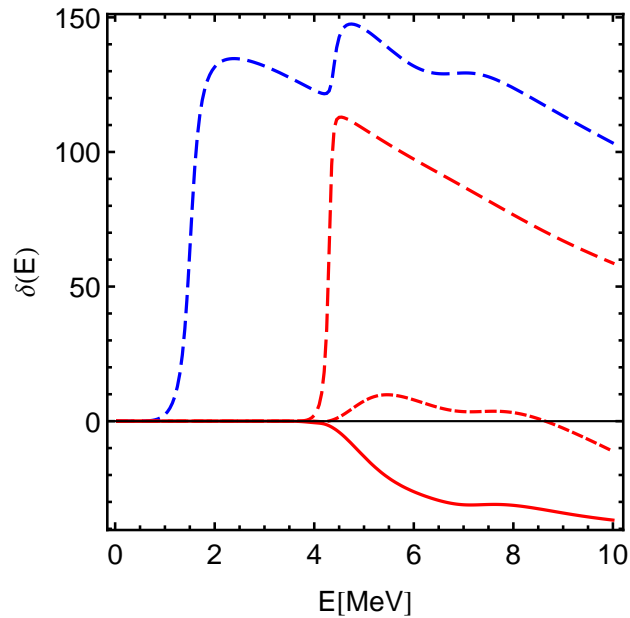
	E [MeV]	$\Gamma_\alpha$ [MeV]	
$0_2^+$	0.29	$1.78 \cdot 10^{-5}$	
$0_3^+$	4.11	0.12	
$0_4^+$	4.76	1.57	(?)

- non-resonant background
- strong coupling between  ${}^8\text{Be}(0^+)$  and  ${}^8\text{Be}(2^+)$  channel at 4.1 MeV
- Hoyle state missed when scanning the phase shifts
- stability of broad resonance with respect to channel radius ?

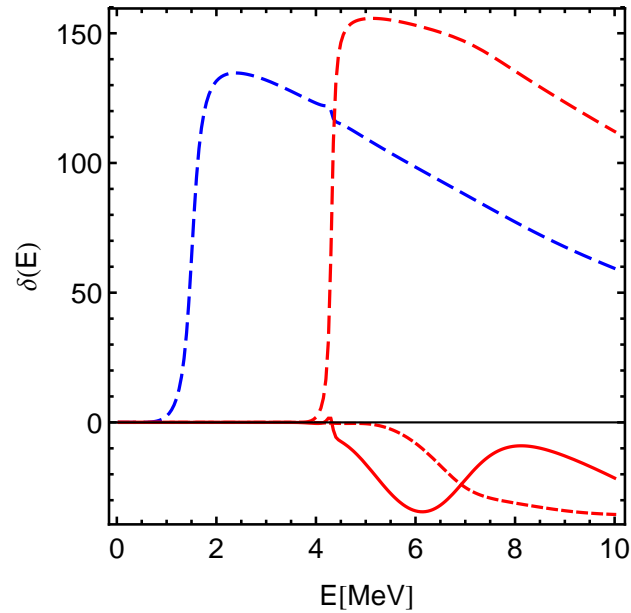
# Cluster Model: ${}^8\text{Be}(0_1^+, 2_1^+)$ - $\alpha$ Continuum

## $2^+$ Phase shifts

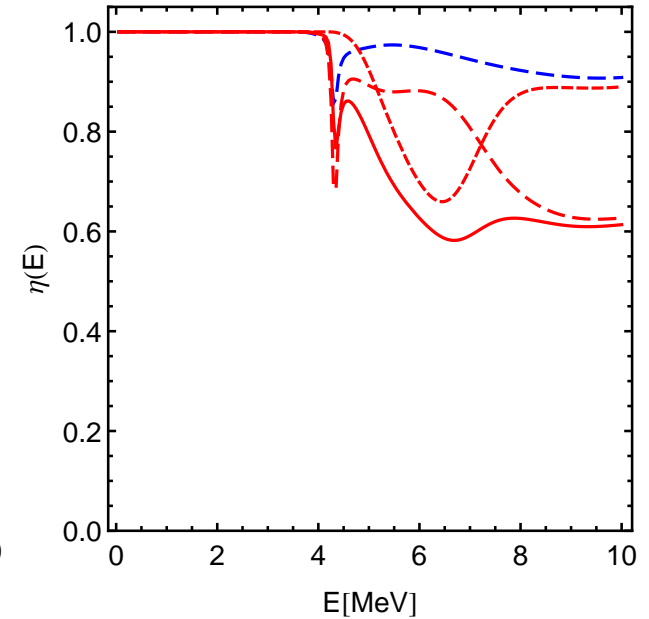
Eigenphaseshifts



Phaseshifts



Inelasticities



Gamow states

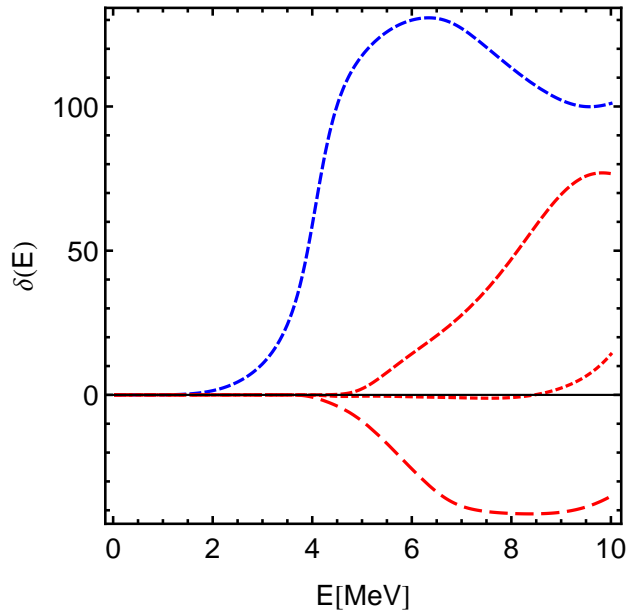
	E [MeV]	$\Gamma_\alpha$ [MeV]
$2_2^+$	1.51	0.32
$2_3^+$	4.31	0.14
...		

- non-resonant background
- $L = 2$   ${}^8\text{Be}(0^+)$  and  ${}^8\text{Be}(2^+)$  resonances

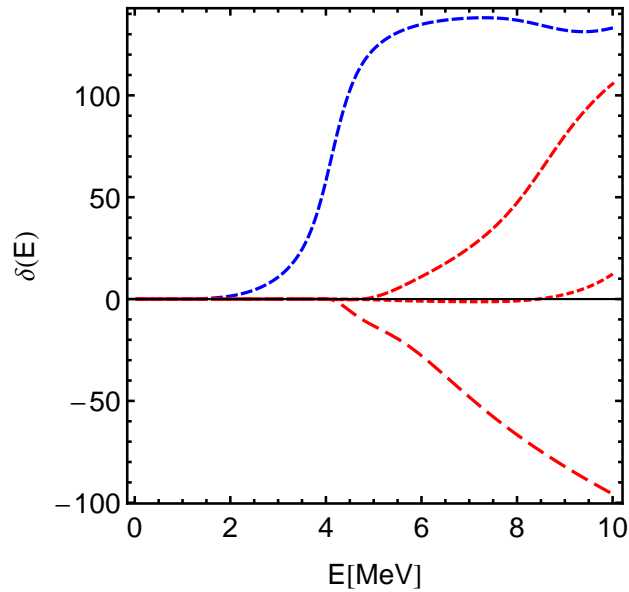
# Cluster Model: ${}^8\text{Be}(0_1^+, 2_1^+)-\alpha$ Continuum

## 4<sup>+</sup> Phase shifts

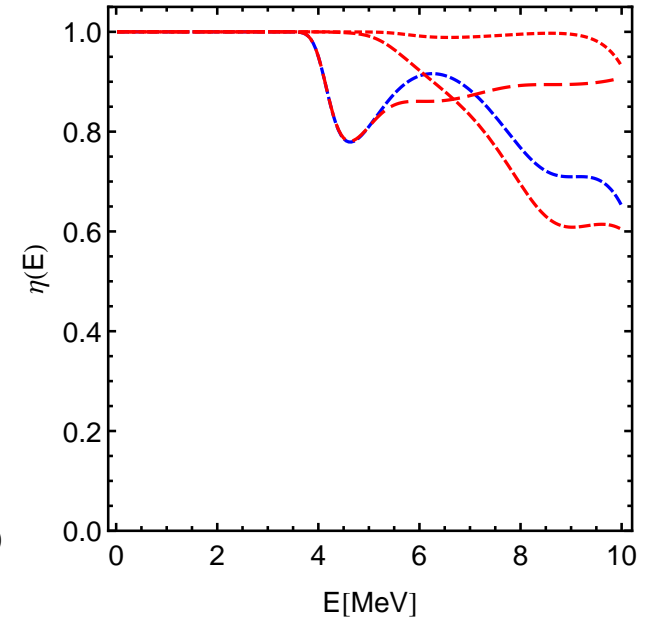
Eigenphaseshifts



Phaseshifts



Inelasticities



Gamow states

	E [MeV]	$\Gamma_\alpha$ [MeV]
4 <sub>1</sub> <sup>+</sup>	1.17	$8.07 \cdot 10^{-6}$
4 <sub>2</sub> <sup>+</sup>	4.06	0.98
...		

- 4<sub>1</sub> state (ground state band) very narrow, missed when scanning phase shifts
- 4<sub>2</sub><sup>+</sup> state mostly  ${}^8\text{Be}(0_1^+)$  but some mixing

# Microscopic $\alpha$ -Cluster Model Including Continuum

	$\rho < 6$ fm $R < 9$ fm	$\rho < 6$ fm $R < 12$ fm	$\rho < 6$ fm $R < 15$ fm	$\rho < 6$ fm Continuum	Experiment
$E(0_1^+)$	-89.64	-89.64	-89.64	-89.64	-92.16
$E^*(2_1^+)$	2.54	2.54	2.54	2.54	4.44
$E^*(0_2^+), \Gamma_\alpha(0_2^+)$	7.82	7.78	7.76	$7.76, 3.04 \cdot 10^{-3}$	$7.65, (8.5 \pm 1.0) \cdot 10^{-6}$
$E^*(2_2^+), \Gamma_\alpha(2_2^+)$	9.18	9.08	8.93	$8.98, 0.46$	$10.13(5), 2.08^{+0.33}_{-0.26}$
$r_{\text{charge}}(0_1^+)$	2.53	2.53	2.53	2.53	2.47(2)
$r(0_1^+)$	2.39	2.39	2.39	2.39	–
$r(0_2^+)$	3.68	3.78	3.89	$4.08 + 0.07i$	–
$B(E2, 2_1^+ \rightarrow 0_1^+)$	9.12	9.08	9.08	9.08	7.6(4)
$M(E0, 0_1^+ \rightarrow 0_2^+)$	6.55	6.40	6.27	$6.02 + 0.01i$	5.47(9)
$B(E2, 2_2^+ \rightarrow 0_1^+)$	2.48	2.09	1.33	$2.11 + 1.41i$	$1.57^{+0.14}_{-0.11}$

- Resonances are calculated as Gamow states
- Matrix elements including resonances are regulated according to Berggren and Gyarmati
- Imaginary part provides information about uncertainty of matrix elements

Berggren, Nucl. Phys. **A109**, 265 (1968)

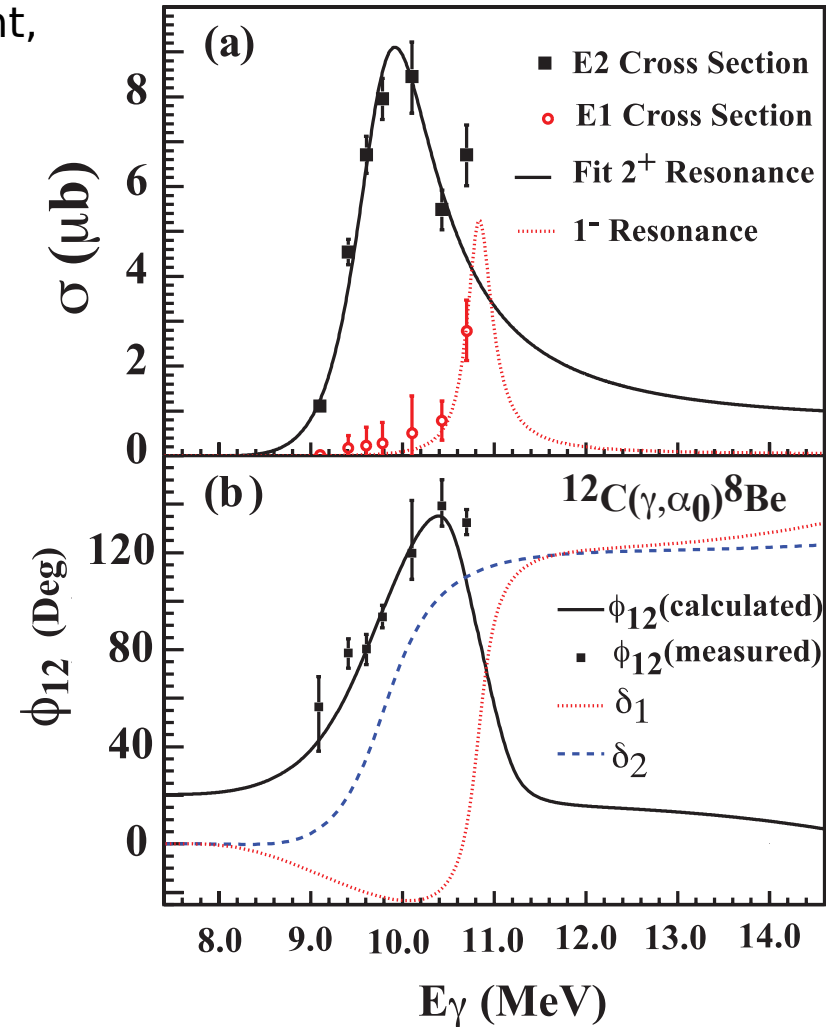
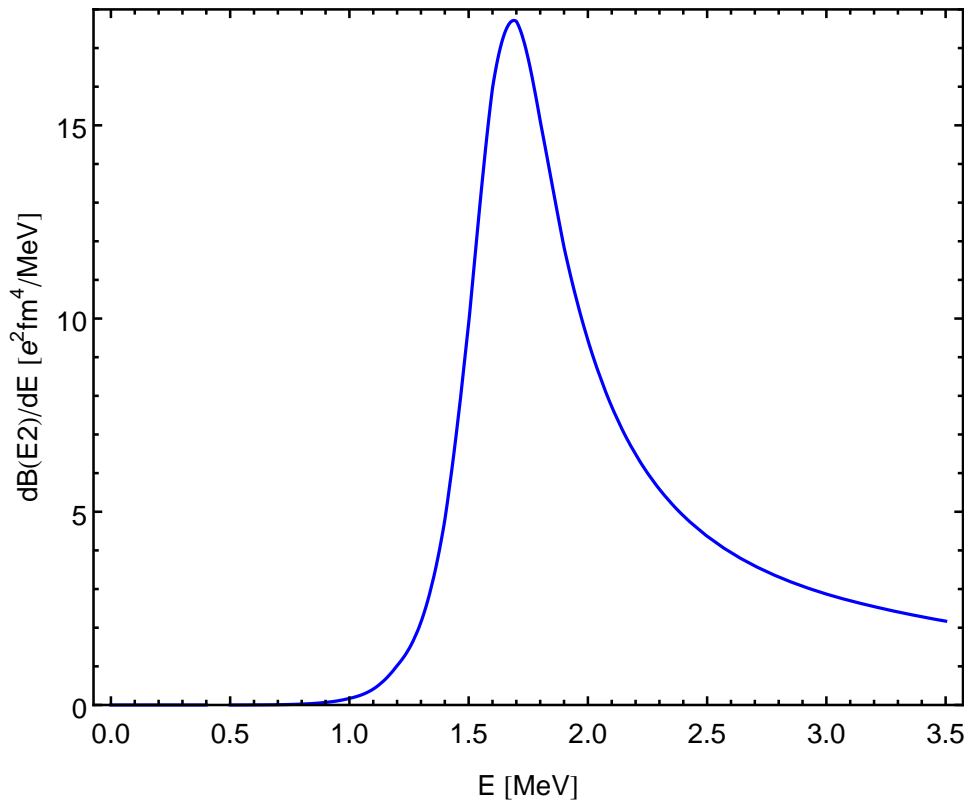
Gyarmati, Krisztinkovics, Vertse, Phys. Lett. **B41**, 475 (1972)

Berggren, Phys. Lett. **B373**, 1 (1996)

# Microscopic $\alpha$ -Cluster Model

## Strength distributions

- Use real continuum (scattering states)
- Might be the better way to compare to experiment, especially for broad and overlapping resonances (background contributions)



Zimmermann et al.,  
Phys. Rev. Lett. **110**, 152502 (2013)



# *Work in Progress:* FMD calculations with $^8\text{Be}$ - $\alpha$ continuum



## **UCOM interaction**

- **Correlation functions from SRG ( $\alpha=0.20 \text{ fm}^4$ ,  $\lambda=1.5 \text{ fm}^{-1}$ )**
- **Increase strength of spin-orbit force by a factor of two to partially account for omitted three-body forces**

## $^8\text{Be}$ - $\alpha$ Continuum

- **To get a reasonable description of  $^8\text{Be}$  it is essential to include polarized configurations**
- ➔ **Calculate strength distributions**
- ➔ **Investigate non-cluster states: non-natural parity states,  $T = 1$  states, M1 transitions,  $^{12}\text{B}$  and  $^{12}\text{N}$   $\beta$ -decay into  $^{12}\text{C}$ , ...**

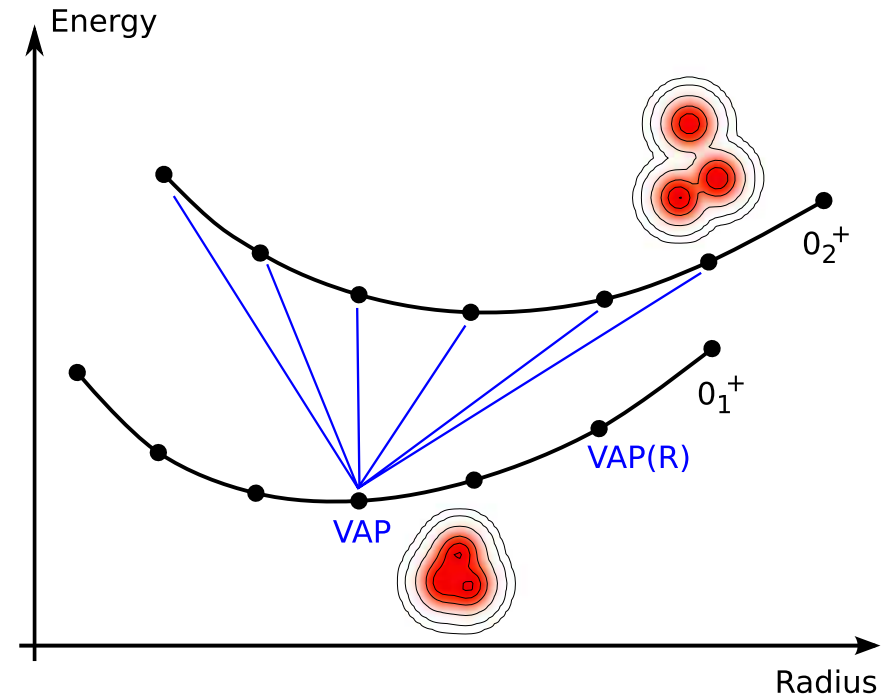
## Model Space

- no assumption of  $\alpha$ -clustering
- complete basis not feasible, find the “most important” basis states
- determine wave packet parameters by variation

## VAP, VAP with constraints, Multiconfiguration-VAP

For each angular momentum ( $0^+$ ,  $1^+$ ,  $2^+$ , ...)

- **VAP**: vary energy of projected Slater determinant  $\tilde{P}^\pi \tilde{P}_{MK}^J |Q(q_i)\rangle$  with respect to all parameters  $q_i$
- **VAP(R)**: create additional basis states by variation with a constraint on the radius of the intrinsic state
- **MC-VAP**: keep VAP state fix and vary the parameters of a second Slater determinant to minimize the energy of the second eigenstate in a multiconfiguration mixing calculation
- **MC-VAP(R)**: create additional basis states by adding a constraint on the radius of the second intrinsic state



# FMD

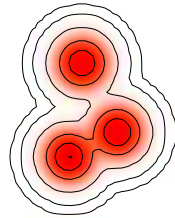
## Important Configurations

- Calculate the overlap with FMD basis states to find the most important contributions to the eigenstates

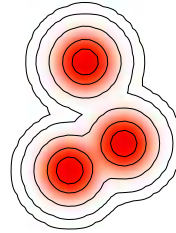


$$|\langle \cdot | 0_1^+ \rangle| = 0.94$$

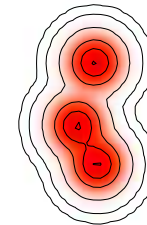
$$|\langle \cdot | 2_1^+ \rangle| = 0.93$$



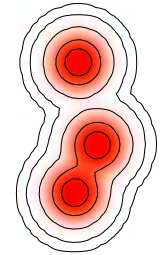
$$|\langle \cdot | 0_2^+ \rangle| = 0.64$$



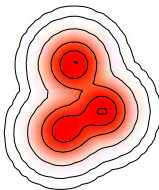
$$|\langle \cdot | 0_2^+ \rangle| = 0.58$$



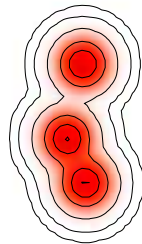
$$|\langle \cdot | 0_2^+ \rangle| = 0.57$$



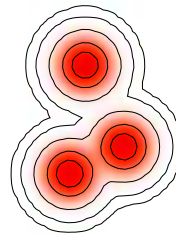
$$|\langle \cdot | 0_2^+ \rangle| = 0.45$$



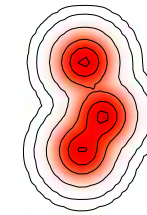
$$|\langle \cdot | 3_1^- \rangle| = 0.91$$



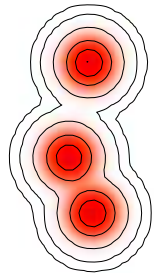
$$|\langle \cdot | 2_2^+ \rangle| = 0.50$$



$$|\langle \cdot | 2_2^+ \rangle| = 0.49$$



$$|\langle \cdot | 2_2^+ \rangle| = 0.44$$

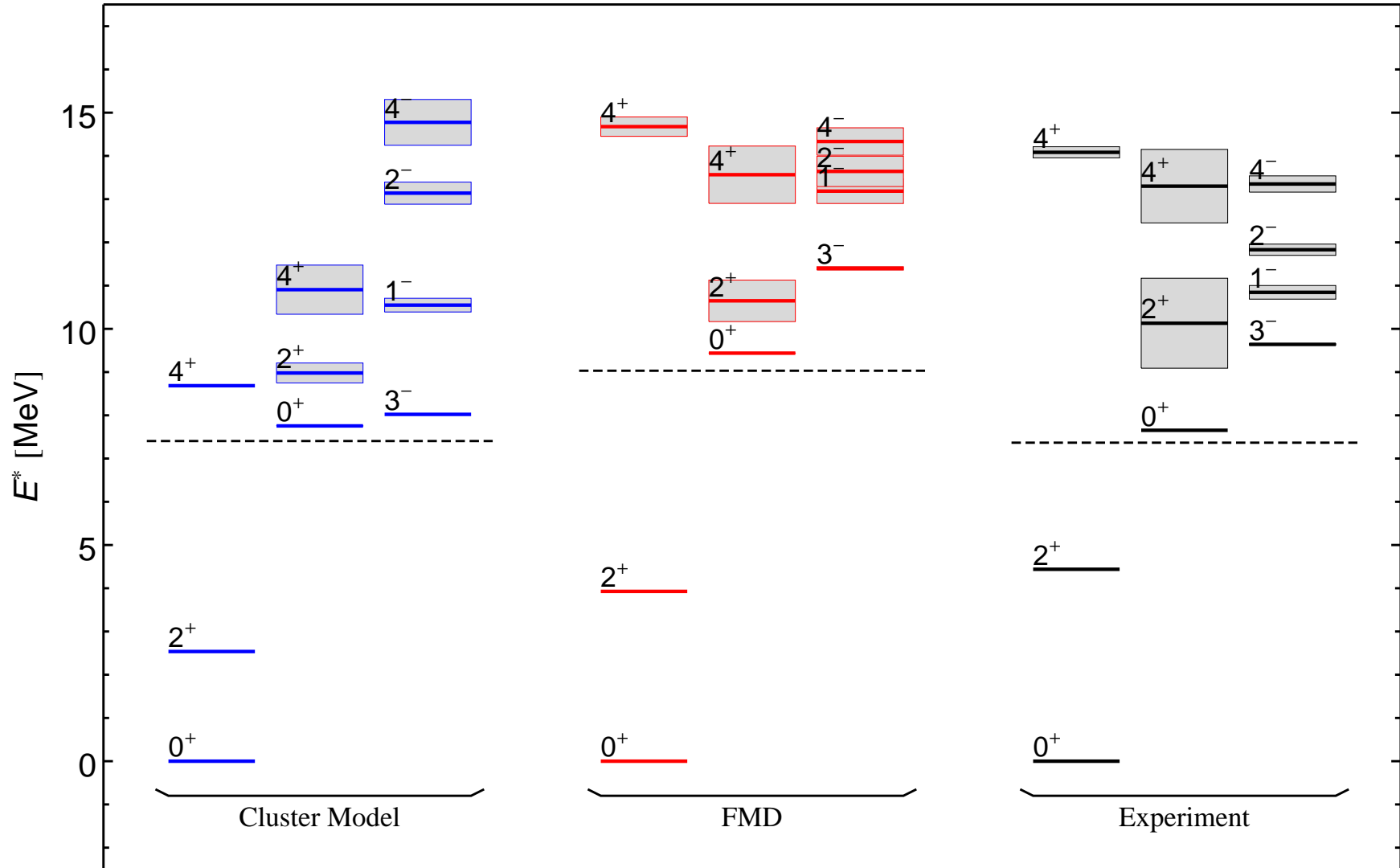


$$|\langle \cdot | 2_2^+ \rangle| = 0.41$$

FMD basis states are not orthogonal!

$0_2^+$  and  $2_2^+$  states have no rigid intrinsic structure

# FMD/Cluster Model: $^8\text{Be}$ - $\alpha$ Continuum Spectra



- FMD:  $^8\text{Be}$  wave functions to be improved

# Summary

## Unitary Correlation Operator Method

- Explicit description of short-range central and tensor correlations

## Fermionic Molecular Dynamics

- Gaussian wave-packet basis contains HO shell model and Brink-type cluster states

## ${}^3\text{He}(\alpha, \gamma){}^7\text{Be}$ Radiative Capture

- Bound states, scattering states, transitions from the continuum

## Microscopic cluster model for ${}^{12}\text{C}$

- Model space with 3  $\alpha$  and  ${}^8\text{Be}-\alpha$  configurations
- Matching with Coulomb continuum, resonances and scattering states
- Hoyle state band build on  ${}^8\text{Be}(\text{gs})-\alpha$

## FMD calculations for ${}^{12}\text{C}$

- VAP and Multiconfig-VAP in internal region,  ${}^8\text{Be}-\alpha$  in external region
- ➔ Investigate EM and GT transitions to the continuum
- ➔  ${}^8\text{Be}-\alpha$  vs real three-body asymptotics ?